ISSN 1075-7015, Geology of Ore Deposits, 2022, Vol. 64, No. 5, pp. 257–280. © Pleiades Publishing, Ltd., 2022.
Russian Text © The Author(s), 2022, published in Geologiya Rudnykh Mestorozhdenii, 2022, Vol. 64, No. 5, pp. 423–450.

The Raduzhnoe Au–Sulfide Deposit (Northern Caucasus): Geological Settings, Mineralogy, and Sources of Metals

E. N. Kaigorodova[a, *], A. V. Chugaev[a], V. A. Lebedev[a], A. S. Sadasyuk[a], B. I. Gareev[b], and G. A. Batalin[b]

[a] *Institute of Geology of Ore Deposits, Petrography, Mineralogy, and Geochemistry, Russian Academy of Sciences Moscow, Moscow 119017 Russia*

[b] *Kazan Federal University, Kazan, 420008 Russia*

**e-mail: katmsu@mail.ru*

Received April 19, 2021; revised February 2, 2022; accepted February 11, 2022

Abstract—The Raduzhnoe Au–sulfide deposit (reserves 4.89 metric tons Au with an average grade of 2.9 ppm), attributed to the intermediate sulfidation epithermal type, is located in the central part of the Bezengi ore district, Northern Caucasus (Khulam–Bezengi gorge, Kabardino-Balkarian Republic). Within this district, Middle Jurassic bimodal moderately alkaline magmatism of the volcano-plutonic Khulam Complex is widespread. The gold-bearing mineralization is confined mainly to fluid-explosive breccias, localized in Jurassic terrigenous sediments, as well as in subvolcanic bodies of the Khulam Complex. The article presents the results of comprehensive petrological–mineralogical and isotope-geochemical studies of gold mineralization of the Raduzhnoe deposit and its host rocks. It was shown that ores at the deposit are represented by polymetallic, Au–sulfide and Au–Ag low-sulfidation assemblages. The last two assemblages are of economic importance. Native gold in ores is low fineness (419–670‰), and associates with sulfides. The main Ag minerals at the deposit are acanthite (Au–Ag low-sulfidation assemblage) and Ag-bearing tetrahedrite-(Zn) and tennantite-(Fe, Zn) (Au–sulfide assemblage). Comparison of Pb isotopic data obtained for ores of the Raduzhnoe deposit and host rocks of different origin indicates that Paleozoic granitoids, representing an "upper crustal reservoir" within the region were the main source of ore lead. The residual felsic melts of the Khulam Complex were a secondary source of lead. According to geochemical data, they are the main source of Ag and Au in ores of the Raduzhnoe deposit. The low Cu and Zn concentrations in felsic rocks indicate that, most likely, the magmatism of the Khulam Complex was not the main source of chalcophile elements in ores of the Raduzhnoe deposit. Presumably, they were extracted from Jurassic ore-bearing terrigenous sediments and metamorphic rocks and granitoids of the Paleozoic basement.

Keywords: Northern Caucasus, gold, Raduzhnoe deposit, sulfide mineralization, Khulam Complex, Jurassic volcanism

DOI: 10.1134/S1075701522040031

INTRODUCTION

Until recently, no large gold deposits were known in the Northern Caucasus, although Au as an associated component is often present in complex polymetallic (Dzhimidon, Sadon, Kakadur-Khanikom), sulfide (Urup, Khudes, Pervomaiskoe, Bykovskoe), and Mo–W (Tyrnyauz) deposits and ore occurrences (*GIS-atlas*, 2020). In 2021, a large deposit named after B.K. Mikhailov (the former Gitche-Tyrnyauz) was put on the balance sheet; the Kurush-Mazinskoe ore field in Dagestan is also promising. This article aims at studying the Raduzhnoe deposit, with its small reserves, but unique for the Greater Caucasus in genesis and type. It is located in the mountainous area of the Kabardino-Balkarian Republic. The deposit was discovered in 1974 (Stativkin et al., 1976(ar)[1]). Based on the results of geological exploration works performed in 2008–2014, the reserves of this deposit are as follows: Au, 4.89 metric tons (C_1, at average grade Au = 2.9 ppm); Ag, 96.4 t (C_1, with an average grade of Ag = 58.99 ppm). The deposit remains poorly studied, and detailed geological, mineralogical, and geochemical information on this deposit is lacking in the scientific literature. In addition, the sources of the mineral-forming ore components are still debatable. Despite the fact that most researchers have suggested a direct genetic association of ore mineralization with Jurassic bimodal volcanism of the Khulam Complex (Lezin et al., 1976(ar); Kalinin et al., 1979(ar); Koptyukh et al., 1985(ar); etc.), these ideas were mainly based on the spatial association of gold-bearing mineralization with hypabyssal rhyolite intrusions. However, there are no published isotope-geochemical data for this deposit that would allow us to give a correct assessment of the role of melts as a source of ore matter.

[1] Hereafter "ar" means archive materials and production reports. A list of stock literature is attached.

The article presents the results of mineralogical, geochemical, and Pb isotope studies of the gold-bearing mineralization of the Raduzhnoe deposit, as well as igneous and sedimentary rocks which are present within the deposit area. The work is based on a study of collections of ore and rock samples gathered by E.N. Kaigorodova during field works over 2011–2020. Based on the results of our research, the mineral compositions of different ore assemblages at the deposit and petrological–geochemical parameters of rocks of the ore-bearing Khulam Complex were established; the origin of ore lead was revealed, and assumptions about sources of other ore components (Au, Ag, Cu, Zn) were made.

SAMPLES AND RESEARCH METHODS

The studied collection includes samples characterizing both the gold-ore mineralization of the Raduzhnoe deposit and the main types of igneous and sedimentary rocks distributed in the area of the deposit. The ore mineralization was studied in 14 samples collected at different sites of the deposit (Pervaya, Orlinaya, Lagernaya, and Kishlyk-su zones) both in exposures and core samples. The host Paleozoic granites, Jurassic sedimentary rocks, and igneous rocks of the Khulam Complex were sampled at the Raduzhnoe deposit, as well as within other sites of the Bezengi ore district (11 samples). Table 1 gives detailed descriptions of the studied samples.

Methods of Studying the Chemical Composition of Rocks and Minerals

The data on the chemical composition of rocks (rock-forming oxides) were obtained y by the X-ray fluorescence at the IGEM-ANALITIKA Center using an Axios mAX (PANalytical) spectrometer (analyst A.I. Yakushev). The contents of rare-earth and trace elements in rocks were determined by inductively coupled plasma ionization mass spectrometry (ICP-MS) on a Thermo XII–Series quadrupole mass spectrometer (IGEM-ANALITIKA Center, analyst Ya.V. Bychkova).

The chemical composition of sulfides and native gold was studied with a JEOL JXA-8200 (EPMA) microprobe analyzer with five wave-dispersive spectrometers (IGEM-ANALITIKA Center, analyst E.V. Kovalchuk) under the following conditions: accelerating voltage 20 kV, current in sample, 20 nA, exposure 10–20 s. The analytical lines are $K\alpha$-line (Cu, Co, Ni, Mn, Fe, S, Zn), $L\alpha$-line (As, Sb, Cd, Mo, Au, Ag, Te, Se, In), and $M\alpha$-line (Pb, Bi, Hg). Pure elements, minerals, and compounds of known composition were used as the standards. Corrections were calculated following the ZAF method using JEOL software. The detection limits were 0.01–0.05 wt %.

The chemical compositions of vein minerals, oxidation zone minerals, and other accompanying minerals were measured by scanning electron microscopy (SEM; JSM-5610LV (JEOL)) with EDS INCA (Oxford Instruments Analytical) using INCA Energy 450 software at the Institute of Geology of Ore Deposits, Petrography, Mineralogy, and Geochemistry, Russian Academy of Sciences (analysts A.V. Mokhov and P.M. Kartashov). The accelerating voltage was 25 keV, the measurement time was 100 s, and the X-ray signal processing time was 6 s. The internal standards were minerals and compounds with a known composition. A matrix correction was introduced with XPP procedure, taking into account the advantages of the ZAF and Phi-Rho-Z methods. The detection limit was ~0.n wt % for light chemical elements and 0.0n wt % for heavy ones.

Pb Isotopic Analysis Method

The Pb isotopic composition was analyzed in microsamples of galena (0.007–0.01 g). The chemical preparation of samples included dissolution of mineral grains in a drop of concentrated nitric acid. Later, the resulting preparation was used to prepare a working solution (3% HNO_3) with Pb content of 200–400 ng/mL. Bulk samples (30–60 mg) of magmatic and metamorphic rocks were decomposed in the mix of concentrated acids HF + HNO_3 (3 : 1) at atmospheric pressure and a temperature of about 130°C for 24 h. Chromatographic separation of Pb was performed following a one-step method (Chugaev et al., 2013) in Teflon microcolumns filled with 0.1 mL of BioRadAG-1×8 anion exchange resin (200–400 mesh size). The analytical blank did not exceed 0.1 ng Pb.

The Pb isotopic composition was measured on a NEPTUNE 9-collector mass spectrometer with inductively coupled plasma according to the method (Chernyshev et al., 2007), which includes correction of the instrumental mass discrimination in lead isotope analysis by the reference isotope ratio $^{205}Tl/^{203}Tl = 2.3889 \pm 1$. The accuracy of the data was controlled by analyzing the Pb isotopic composition in the SRM-981 isotopic standard and standard reference rock samples AGV-2 and BCR-1 of USGS. The total errors (±2SD) of measuring $^{206}Pb/^{204}Pb$, $^{207}Pb/^{204}Pb$, and $^{208}Pb/^{204}Pb$ ratios did not exceed ±0.02% for galena, and ±0.03% for whole rock.

For age-correction the measured Pb ratios in rocks, the Pb, Th, and U contents were measured in the same samples using inductively coupled plasma mass spectrometry on an iCAP Qc ICP-MS (Thermo Scientific) at the Laboratory of Isotope and Elemental Research of IGPT KFU. The error in determining the Pb, Th, and U contents in samples, estimated from the results of systematic analyses of standard rock samples BHVO-2 and AGV-2 of USGS, did not exceed ±3% (±2SD).

Table 1. Characteristics of studied samples from Bezengi ore district

Sample	Sampling sites (system of coordinates WGS84)	Characteristics
3001/2	Borehole 3001 (int. 69.0 m). Pervaya ore zone (43°14′19.8″ N 43°18′13.4″ E)	Fluid-explosive mudstone breccia with carbonate–barite cement (gold–silver low-sulfidation assemblage)
3001/4	Borehole 3001 (int. 83–84 m). Pervaya ore zone (43°14′19.8″ N 43°18′13.4″ E)	Massive sulfide ore with a carbonate veinlet (gold–silver assemblage)
3001/5	Borehole 3001 (int. 84–87 m). Pervaya ore zone (43°14′19.8″ N 43°18′13.4″ E)	Siltstone with sulfide pockets (pyrite, chalcopyrite) (gold–silver assemblage)
3001/7	Borehole 3001 (int. 93–99 m). Pervaya ore zone (43°14′19.8″ N 43°18′13.4″ E)	Fluid-explosive mudstone breccia with quartz-carbonate cement and sulfides (gold–silver assemblage)
3001/12	Borehole 3001 (int. 126 –132 m). Pervaya ore zone (43°14′19.8″ N 43°18′13.4″ E)	Quartz–sulfide vein in granites of Belorechensk Complex (polymetallic assemblage)
RTs-7	Kishlyk-su zone (43°13′44.9″ N 43°16′10.3″ E)	Sandstones of Dghigiat Formation with intensive carbonate-sulfide mineralization (gold–silver assemblage)
R-12	Trench 407. Kishlyk-su zone (43°13′46.1″ N 43°16′12.6″ E)	Silicified siltstones with barite-sulfide veinlets (gold–silver assemblage)
R-17	Borehole 3008. Pervaya ore zone (43°14′21.9″ N 43°18′18.9″ E)	Fluid-explosive silicified mudstone breccia with quartz-sulfide cement (gold–silver assemblage)
R-18	Borehole 3010. Pervaya ore zone (43°14′20.0″ N 43°18′16.3″ E)	Fluid-explosive silicified mudstone breccia with quartz-sulfide cement (gold–silver assemblage)
R-23	Borehole 3061, Kushkhule-su R., Lagernaya zone (43°14′13.0″ N 43°17′52.8″ E)	Quartz-sphalerite-galena veinlet in silicified sandstones (polymetallic assemblage)
3/2-210	Orlinaya zone (43°14′25.8″ N 43°16′29.3″ E)	Sandstone (Pliensbachian Stage, Bezengi Formation) silicified with superimposed sulfide mineralization (polymetallic assemblage)
3/2-181	Orlinaya zone (43°14′25.8″ N 43°16′29.3″ E)	Argillized rhyolite (Khulam Complex) with superimposed dolomite-quartz-sulfide mineralization (gold–silver assemblage)
2/3-187	Orlinaya zone (43°14′00.4″ N 43°16′12.6″ E)	Argillized rhyolite (Khulam Complex) with sulfide veinlets (gold–silver assemblage)
Kh-2	Khulam sill (43°14′24.7″ N 43°18′31.9″ E)	Fluidal argillized rhyolite, Khulam Complex with sulfide mineralization (galena)
RTs-3	Pervaya ore zone (43°13′58.4″ N 43°18′21.4″ E)	Granite (Belorechensk Complex) sericitized greenish white with sulfide assemblage
3001/6	Borehole 3001 (int. 87–88 m). Pervaya ore zone (43°14′19.8″ N 43°18′13.4″ E)	Mudstone (Aalenian Stage, Dzhigiat Formation) with a net of gypsum veinlets
210-1/13	Kardan ore field (43°14′49.0″ N 43°12′27.8″ E)	Argillized rhyolite, Khulam Complex
210-2/13	Kardan ore field (43°14′46.9″ N 43°12′34.5″ E)	Rhyolite, Khulam Complex
R-6	Pervaya ore zone (43°14′21.8″ N 43°17′54.7″ E)	Eruptive rhyolite breccia with rhyolite cement
R-10	Pervaya ore zone (43°14′22.6″ N 43°18′26.3″ E)	Eruptive breccia of argillized rhyolites
210-5/13	Kardan ore field (43°15′02.3″ N 43°12′29.7″ E)	Trachyandesibasalt (mugearite), Khulam Complex
R-19	Mt. Mukol-kaya, lower sill (43°12′33.2″ N 43°16′02.0″ E)	Gabbro, Khulam Complex
B-3	Shtulu-Kharess depression, Khulam-Bezengi gorge (43°04′26.0″ N 43°04′49.2″ E)	Black shale, Pliensbachian–Toarcian (Galiat Formation)
KS-A	Northern Jurassic depression, Khulam-Bezengi gorge. Raduzhnoe deposit, Kishlyk-su site (43°14′00.4″ N 43°16′12.6″ E)	Black shale, Aalenian (Dzhigiat Formation)
D-1	Dumala depression, Khulam-Bezengi gorge. Dumala River valley (43°08′26.9″ N 43°16′32.2″ E)	Black shale, Pliensbachian–Toarcian (Bezengi Formation)

GEOLOGICAL DESCRIPTION OF THE STUDY AREA

The Raduzhnoe deposit is located in the central part of the Bezengi ore district (Fig. 1). The Paleozoic basement of the region belongs to the tectonic zone of the Greater Caucasian Range (Balkarian-Digorian block) and consists of crystalline schists, gneisses, granite-gneisses, and amphibolites intruded by Devonian–Carboniferous granitoids (Somin, 2011), as well as Middle Jurassic diabase dikes of the Kazbek Complex in the southern part of the region (Kurbanov et al., 2004(ar)). The basement has a block structure; horst uplifts are separated by longitudinal tectonic depressions of general Caucasian direction (Dumala, Northern Jurassic). The latter are filled with Early–Middle Jurassic sedimentary rocks (sandstones, mudstones, siltstones, shales). The largest tectonic faults are NW–SE-trending Saugam and Saurdan fault systems; the latter controls the manifestation of Mesozoic moderately alkaline magmatism, predominantly in the sedimentary cover of the Northern Jurassic depression. According to the results of multi-year geological research conducted in the XX century (Lebedev, 1950; Gorokhov et al., 1968(ar); etc.), presumably Middle Jurassic moderately alkaline magmatic formations, common in the deposit area, were identified as a separate Khulam volcano-plutonic complex (Dolgikh, 1978). The area of maximum distribution of igneous formations of this complex is located in the mountainous part of Balkaria between Chegem–Cherek Bezengiisky and Cherek Bezengiisky–Cherek Balkarsky watersheds; further to the southeast and northwest, the number of hypabyssal intrusions exposed due to erosion gradually decreases (Fig. 1).

Our U–Pb datings obtained for zircons from rhyolites and trachytes (167 ± 4 Ma and 167 ± 3 Ma, respectively) indicate the time of emplacement of felsic and moderately felsic magmatic formations of the Khulam Complex (Kaigorodova and Lebedev, 2022). The probable age is estimated as Bajocian–Callovian (Cohen et al., 2020). K–Ar dating of the monomineral phlogopite fraction from gabbroids of the Kardan River valley confirm the Middle Jurassic age of mafic rocks of the Khulam Complex (Kaigorodova and Lebedev, 2022).

Neogene–Quaternary igneous rocks with various compositions distributed to the south and west of the Bezengi ore district belong to three different complexes (Kaigorodova et al., 2021). The Pliocene (4.7 Ma) Tsana Complex includes trachyandesibasalt dikes in the Dumala River valley. Pyroclastic rocks (ignimbrites and tuffs) of the Late Pliocene Chegem Complex (about 3 Ma) are found on the westernmost periphery of the area. On the Cherek Bezengiisky–Cherek Balkarsky watershed, in the area of Mt. Cheget-Dzhora, there are remnants of the Pleistocene (about 700 ka) Udursu andesite flow, conditionally assigned to the Elbrus Complex.

Tectonic Settings

The main tectonic structures of the area are NW–SE-trending faults (southern and northern branches of the Saurdan system, Fig. 2), which are considered the main ore-controlling structures of the Bezengi ore district and melt-feeder structures for volcanic rocks of the Khulam Complex. In the area of the Raduzhnoe deposit, there are also submeridional faults (Bodulinsky and Gipsovy), which apparently were local magma-feeder structures, because they are associated with the root zones of two large laccolith-like structures of the Khulam Complex (Orlinaya Zone and Vtoraya Ore Zone), crosscut by exploration boreholes.

GEOLOGICAL STRUCTURE OF THE RADUZHNOE DEPOSIT

Host Rocks

The Raduzhnoe deposit is located on the left side of the Khulam–Bezengi gorge at an altitude of 1900–2300 m in the area where Paleozoic basement formations (granitoids of the Belorechensk Complex γPZ_3bl) have subsided beneath a cover of Early–Middle Jurassic terrigenous formations (Fig. 2). The granitoids are mainly represented by coarse- and medium-grained two-mica and biotite varieties.

The Jurassic sedimentary rocks in the area of the Raduzhnoe deposit are represented by sandstones, mudstones, and siltstones of the Pliensbachian, Toarcian, Aalenian, and Bajocian ages. According to the accepted regional stratigraphic scheme of the area (Beznosov et al., 1973), they are subdivided into three formations (from bottom to top): Bezengi, Dzhigiat, and Dzhora.

The volcanic rocks of the Khulam Complex that break through the Lower–Middle Jurassic sedimentary strata belong to the gabbro–trachyandesibasalt–trachyte–rhyolite contrast-differentiated bimodal assemblage (Kaigorodova and Lebedev, 2022). Rhyolites and trachytes are the most widespread in the deposit area, which mainly make up sill- and laccolite-like subvolcanic bodies (at the Orlinaya, Kishlyk-su, and Vtoraya ore zones), necks (Saurdan Fault Zone, Fig. 3c), and complex multiactive intrusion structures. The largest structure among them is the so-called Khulam sill (Fig. 3b). Its thickness and length are 200 m and 4.5 km, respectively. Mafic rocks (basaltoids) making up small subvolcanic bodies are less widespread (Fig. 3a).

Petrographic Description of the Khulam Complex Rocks

Rhyolites are represented by two varieties: aphyric (white and whitish gray) and porphyritic (light gray to gray). Phenocrysts in porphyritic rocks amount to 3–10%; orthoclase dominates, while sanidine is less common. The structure of rhyolites is massive or flu-

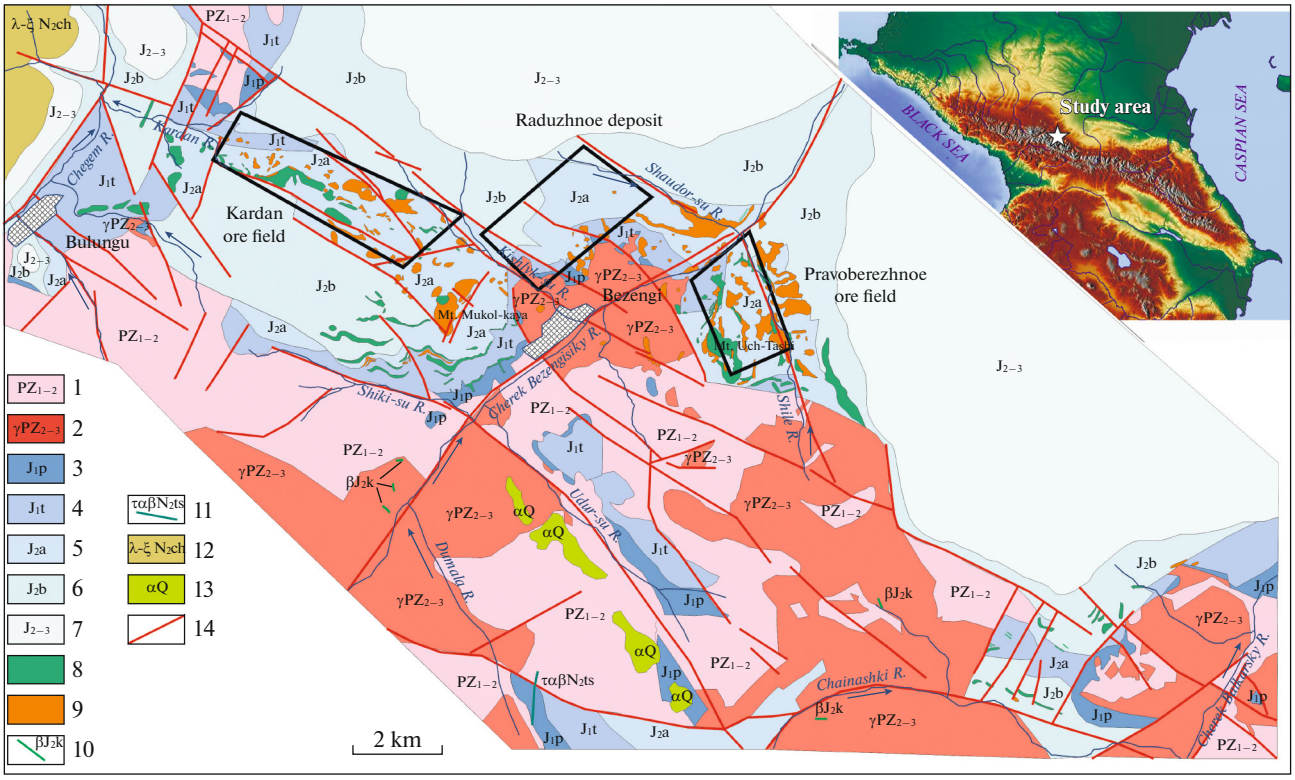

Fig. 1. Schematic geological map of Bezengi ore district with outlines of Raduzhnoe deposit and potential ore fields (Kardan and Pravoberezhnoe), compiled based on materials from (Kachurin et al., 1991(ar); Pismenny et al., 2002(ar); Kaigorodova et al., 2021). (1) Paleozoic metamorphic complexes (gneisses, crystalline schists, amphibolites), (2) Middle Late Paleozoic granitoids, (3–6) sedimentary rocks of Northern Jurassic depression ((3) Pliensbachian Stage, (4) Toarcian Stage, (5) Aalenian Stage, (6) Bajocian Stage), (7) undivided Middle–Late Jurassic formations of Skalisty Ridge zone, (8–9) igneous rocks of Middle Jurassic Khulam Complex ((8) mafic, (9) felsic and moderately felsic rocks), (10) dikes of Middle Jurassic Kazbek Complex (diabases, gabbroids), (11) magmatic formations of Pliocene Tsana Complex (trachyandesibasalts), (12) Pliocene rhyolite ignimbrites of Chegem Complex, (13) Pleistocene andesites of Elbrus Complex, (14) major faults.

idal. Felsitic groundmass of aphyric and porphyritic rhyolites is composed of microcrystalls of plagioclase (30–35 vol %), potassium feldspar (up to 10–15 vol %) and quartz (35–60 vol %). The glass of the matrix is completely altered by minerals of the illite–smectite group and kaolinite. Rhyolites of the Khulam Complex contain 68.2–84.6 wt % SiO_2[2], 2.3–12.3 wt % $K_2O + Na_2O$ (at 0.3–12.1 wt % K_2O) and are attributed to the moderately alkaline and calc-alkaline petrochemical series (Fig. 4). They are characterized by substantial variations in the SiO_2/total alkali ratio, as well as the SiO_2/K_2O and K_2O/Na_2O ratios. The latter parameter can be used to separate rhyolites into four subgroups: ultra-potassic ($K_2O/Na_2O > 40$), high-potassic (K_2O/Na_2O from 15 to 40), potassic (K_2O/Na_2O from 2 to 15), and low-potassic ($K_2O/Na_2O < 2$) (Kaigorodova and Lebedev, 2022).

Trachytes are pinkish gray, pinkish green, often spotted. They include a large number of phenocrysts of dark pink potassium feldspar. According to (Borsuk et al., 1977), it is nonmeshed microcline that developed after primary orthoclase. The texture of trachytes is glomerophyric with the trachytic texture of the groundmass. Trachytes of the Khulam Complex contain 59.7–65.5 wt % SiO_2, 7.7–12.2 wt % $K_2O + Na_2O$ (at 2.1–7.2 wt % K_2O) and are attributed to the moderately alkaline petrochemical series (Fig. 4). These are highly differentiated (Mg# from 0.19 to 0.55, Ni < 20 ppm, Cr < 25 ppm, and Co < 20 ppm) formations; according to the K_2O/SiO_2 ratio, they are high-potassic.

Mafic rocks of the Khulam Complex, widespread in the flanks of the deposit, are represented by massive holocrystalline gabbro (small-, medium- and coarse-grained), and rarely intensively altered basaltoids.

Metasomatic Alterations of Host Rocks

Based on our geological observations, petrographic study of thin sections, and mineral composition study of mixed-layer mineral phases from metasomatically altered rocks using X-ray diffraction, the preore and synore stages of development of metasomatic formations were identified at the Raduzhnoe deposit. The

[2] The contents of rock-forming oxides are normalized to 100%.

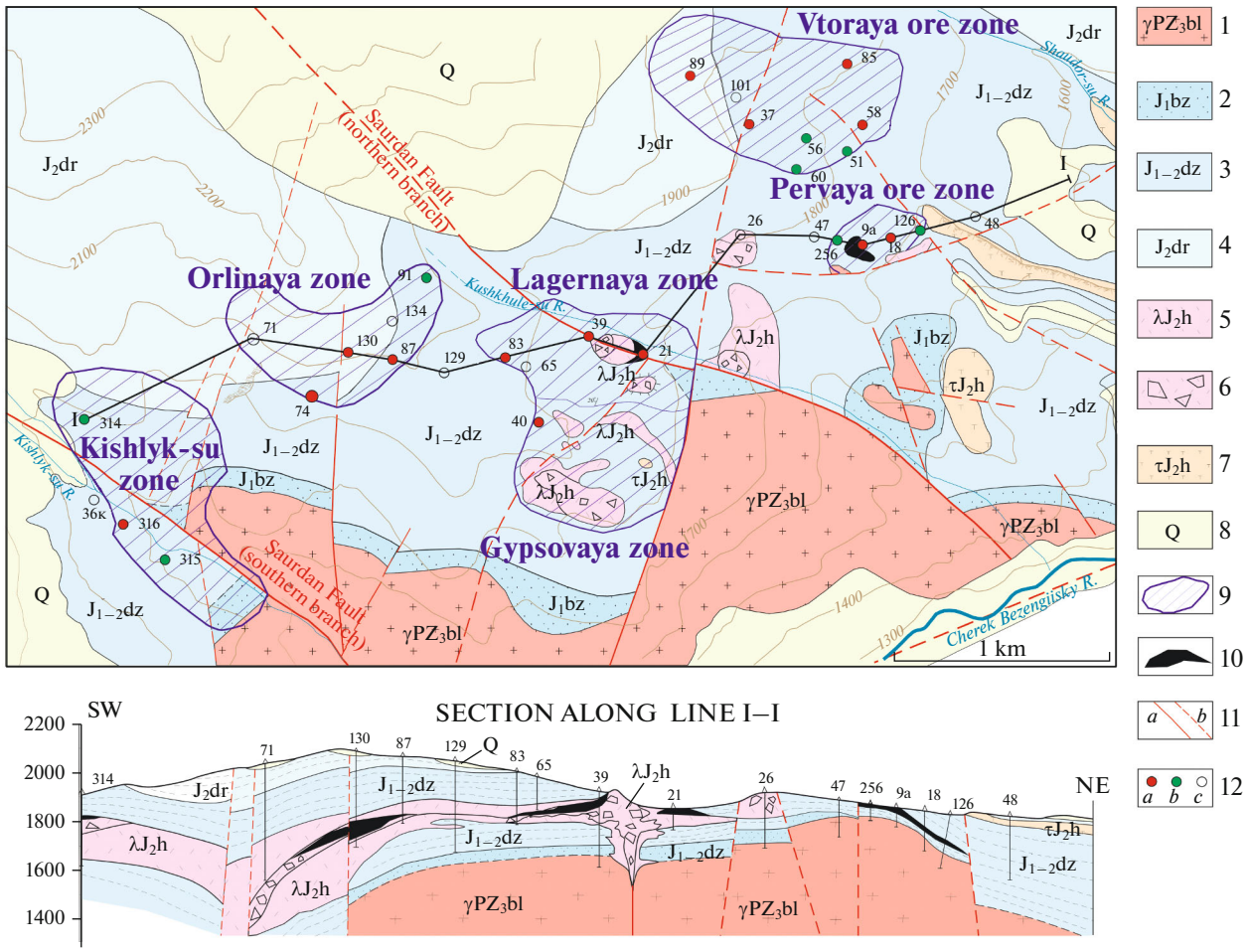

Fig. 2. Schematic geological map with contours of ore zones and cross-section of Raduzhnoe deposit. Map is compiled based on materials from (Kachurin et al., 1991(ar); Platkov et al., 1991(ar)). (1) granitoids of Belorechensk Complex (Early-Middle Carboniferous); (2–4) Jurassic sedimentary cover ((2) Bezengi Formation, (3) Dzhigiat Formation, (4) Dzhora Formation); (5) rhyolites of Khulam Complex; (6) vent facies of rhyolites; (7) trachytes of Khulam Complex; (8) Quaternary sediments; (9) contours of hidden orebodies; (10) orebodies in section and on surface; (11) faults ((*a*) established, (*b*) proposed); (12) exploration boreholes and its number ((*a*) Au >1 ppm; (*b*) Au 0.5–1 ppm; (*c*) Au <0 ppm).

preore stage is characterized by widespread low-temperature propylitic alteration (epidote-free chlorite propylites) in the entire development zone of volcanic rocks of the Khulam Complex (Chegem-Cherek Bezengiisky and Cherek Bezengiisky-Cherek Balkarsky watershed), as well as aerial silicification within the fault zones of the Saurdan system.

The preore stage is manifested more locally in the central part of the Bezengi ore district (Raduzhnoe deposit, Kardan and Pravoberezhnoe ore fields) and are characterized by a wide distribution of argillizated rocks. Based on the generally accepted ideas (*Metasomatism* ..., 1998), we assume that the solutions at this stage were near-neutral and were characterized by a high silica content and higher potassium contents.

The synore stage is manifested by the local development of superimposed silification (quartz, as a rule, is chalcedony-like) and carbonatization of ore-hosting rocks. Metasomatic carbonates are represented by calcite, Fe-dolomite, dolomite, and siderite.

Orebodies

The Raduzhnoe deposit includes several spatially adjacent orebodies, distinguished as separate sections or ore zones (Fig. 2). They are diverse in their morphology, but mainly lenticular in section and isometric in plan view.The dimensions of the orebodies delineated by a gold cutoff grade of 0.5 ppm are characterized by the following parameters (according to (Baranovsky et al., 2014(ar)): Pervaya ore zone (365 × 60 m) in plan, occurrence depth from 0 to 155 m, average thickness 17 m; Gypsovaya zone (two orebodies) 135 × 95 m, occurrence depth from 0 to 19.0 m, average thickness 4.4 m and 155 × 65 m, occurrence depth from 3.0 to 25.5 m, average thickness 4.7 m; Lagernaya Zone 95 × 35 m, occurrence depth from 0 to 17.0 m,

average thickness 12.5 m. The orebodies occurring within rhyolite sills are 330 × 240 m with an average thickness of 4.3 m and depths from 204 to 376 m (Orlinaya Zone).

Ore mineralization at the Raduzhnoe deposit is confined to cement and fragments of fluid-explosive breccias occurring in the host Jurassic terrigenous strata and volcanic rocks of the Khulam Complex. In connection with the processes of mid-Jurassic tectonomagmatic activation, breccias of different origin developed within the Bezengi ore district: tectonogenic (Fig. 5a), eruptive magmatic (Figs. 5b, 5c), and fluid-explosive hydrothermal (Figs. 5d–5f). Eruptive magmatic breccias are widespread both at exocontacts of subvolcanic bodies of felsic and moderately felsic volcanic rocks, represented by angular fragments of rhyolites and trachytes, enclosed in intensely deformed sedimentary rocks, and in the central parts of complicated subvolcanic structures. Fluid-explosive hydrothermal breccias with ore mineralization often overlie eruptive breccias. Fluid-explosive breccias form irregularly shaped pipes and lenticular interbedded bodies in zones of host rocks with maximum permeability. The fluid-explosive hydrothermal breccias of the Raduzhnoe deposit can be classified (Sharpenok et al., 2018) as fluidogenic cryptoexplosive breccias, which are of the greatest economic interest because they are usually ore-bearing.

The fluid-explosive breccias of the Raduzhnoe deposit are characterized by extreme heterogeneity in the composition of clasts and cement. Clasts are represented by silicified mudstones, siltstones, sandstones, felsic volcanic rocks, and rarely sulfide ores. The cement is carbonate–siliceous, quartz (Fig. 5d), carbonate–barite (Fig. 5e), hematite (Fig. 5f), and rarely sulfide. Signs of multiple brecciation are present; no sorting of rock fragments by size is observed. Ore mineralization is localized both in the cement of breccias and in rock fragments.

The Au grade in ores varies from 0.1 to 215 ppm; Ag, from 1 to 4000 ppm. The main ore minerals are native gold and silver, acanthite, pyrite, galena, sphalerite, chalcopyrite, and fahlore. Native gold is usually found in association with chalcopyrite or galena (Fig. 11).

Within orebodies, mineralization is extremely irregularly developed. Therefore, the reserves were assessed taking into account the ore content coefficient, which was 0.83 for the richest ore blocks (Kalinin et al., 1979(ar)).

Based on previous studies (Mezenina et al., 1982(ar)), polymetallic mineralization was established in all sections of the deposit, reaching a total polymetallic content from 1.0 to 21.2 wt % in boreholes of the Pervaya ore zone; in a separate assessment: Pb content, up to 6.5 wt %; Zn, up to 17.2 wt %, and Cu, up to 5.8 wt %. Given the insufficient degree of knowledge about the associated components, Cu, Pb, and Zn resources at the Pervaya, Gypsovaya, and Lagernaya ore zones are taken into account as noneconomic predicted (thous. t): Cu, 5.96, Zn, 12.55; Pb, 8.57 (Baranovsky et al., 2014(ar)).

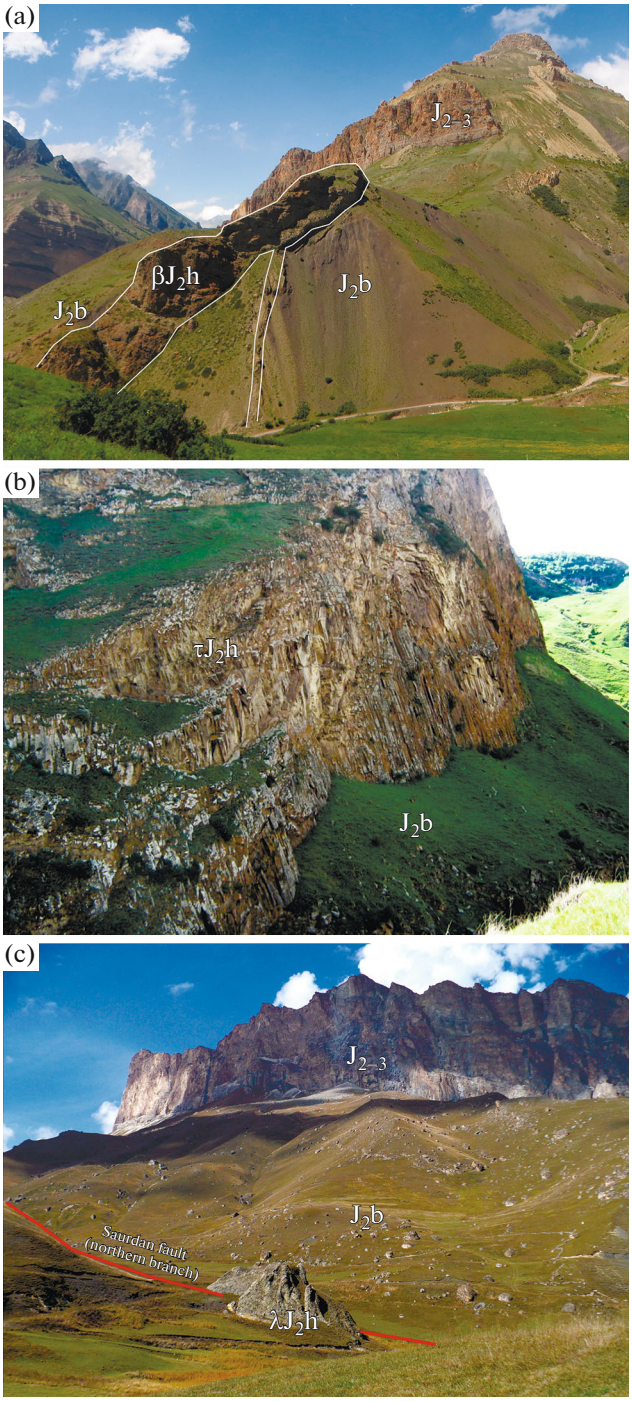

Fig. 3. Outcrops of volcanic rocks of Khulam Complex within Bezengi ore district. (a) basaltoid sill of Khulam Complex with a feeding dike, right bank of Kardan River; (b) Khulam sill (trachytes and rhyolites); (c) rhyolite neck in Saurdan Fault zone, Lagernaya ore zone ((a) images by E.N. Kaigorodova, (b, c) images by V.P. Davidenko).

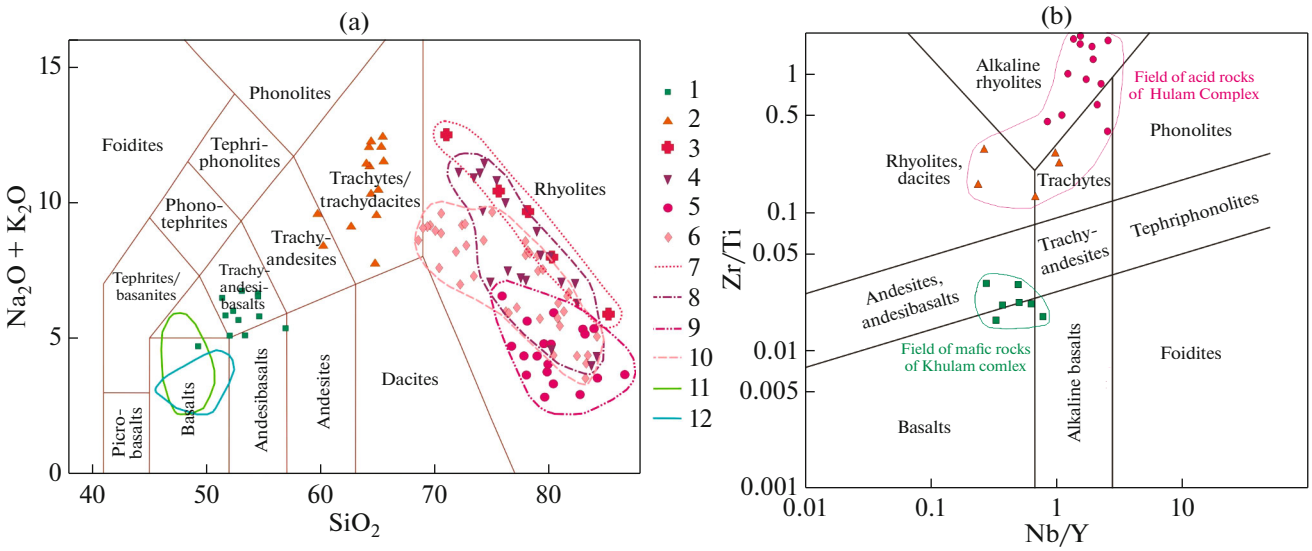

Fig. 4. Classification petrological diagrams for studied igneous formations of Khulam Complex (author's data; data from following studies: Gazeev et al., 2019; Gorokhov et al., 1968(ar); Grigorchuk et al., 1980(ar); Davidenko et al., 1993(ar); Kalinin et al., 1979(ar); Koptyukh et al., 1985 (ar); Spassky et al., 1982(ar)). (a) SiO_2–Na_2O+K_2O (Le Bas et al., 1986), (b) Nb/Y–Zr/Ti (Pearce, 1996). (1) mafic igneous rocks of Khulam Complex; (2) trachytes of Khulam Complex; (3–6) rhyolites of Khulam Complex ((3) ultra-potassic, (4) high-potassic, (5) moderately potassic, (6) low-potassic); (7–10) fields of different types of rhyolites of Khulam Complex ((7) ultra-potassic, (8) high-potassic, (9) moderately potassic, (10) low-potassic); (11) field of igneous rocks of Middle Jurassic Kazbek Complex (Gazeev et al., 2018); (12) field of igneous rocks of Early Jurassic Fiagdon Complex (Gurbanov et al., 2017).

The age of the Raduzhnoe deposit is based on geological data—spatial relationship of ore-bearing fluid-explosive breccias with rhyolite sills and necks of the Khulam Complex. This provided the basis for previous researchers to suggest the synchronous development of ore formation and Middle Jurassic volcanism (Lezin et al., 1976(ar); Koptyukh et al., 1985(ar)).

Ore Textures and Structures

The ores have massive, spotted, disseminated (Fig. 6c), veined, and breccia structures. The structures of ores usually depend on the structure and ratio of different mineral aggregates and host rocks. Vein structures (Figs. 6d, 6h) are typical of ores localized in granites. Breccia structures (Fig. 6b) are the most common because of the widespread development of fluid-explosive breccias at the deposit.

No metacolloid or banded structures typical of classical LS-type Au–Ag epithermal deposits have been found at the Raduzhnoe deposit.

The ore textures are usually equigranular; sometimes there are crumple structures clearly distinguishable in galena. In Au–sulfide ores, cockade structures are observed only in thin sections (Fig. 8c).

MINERAL COMPOSITION OF ORES

The ores of the Raduzhnoe deposit consist of three mineral assemblages, the distribution of which is vertically zoned. The mineral compositions of the identified ore assemblages are shown in Table 2.

(1) The Au–Ag low-sulfidation assemblage formed by barite and carbonates with acanthite, native gold, galena, sphalerite, and chalcopyrite occurs in the upper horizons composed of the fluid-explosive breccias. This assemblage has an extremely limited distribution within the deposit and was described only in the central part (Pervaya ore zone).

(2) The Au–sulfide assemblage is characteristic for orebodies spatially associated with subvolcanic bodies—laccoliths and rhyolite sills. In addition to polymetallic mineralization, chalcopyrite and gold, pyrite and sulfosalts are common here. Vein minerals are represented by quartz, barite, gypsum, and anhydrite.

(3) The polymetallic (galena–sphalerite–chalcopyrite) assemblage is localized in basement granites and Lower Jurassic sandstones of the Bezengi Formation. This assemblage contains no economic gold content (the grade does not exceed 0.2–0.8 ppm). The ore minerals are galena, sphalerite, chalcopyrite, and pyrite; the vein minerals are quartz and barite.

Based on prospecting and exploration results (Mezenina et al., 1982(ar)), the Au–Ag low-sulfidation and Au–sulfide mineral assemblages were found to be economic (Au contents >0.5 g/t).

In total, 40 different minerals (including hypergene minerals and minerals of metasomatically altered host rocks, such as sericite, illite-smectite, and kaolinite) were found in the ores of the Raduzhnoe deposit. The most common minerals at the Raduzhnoe deposit are

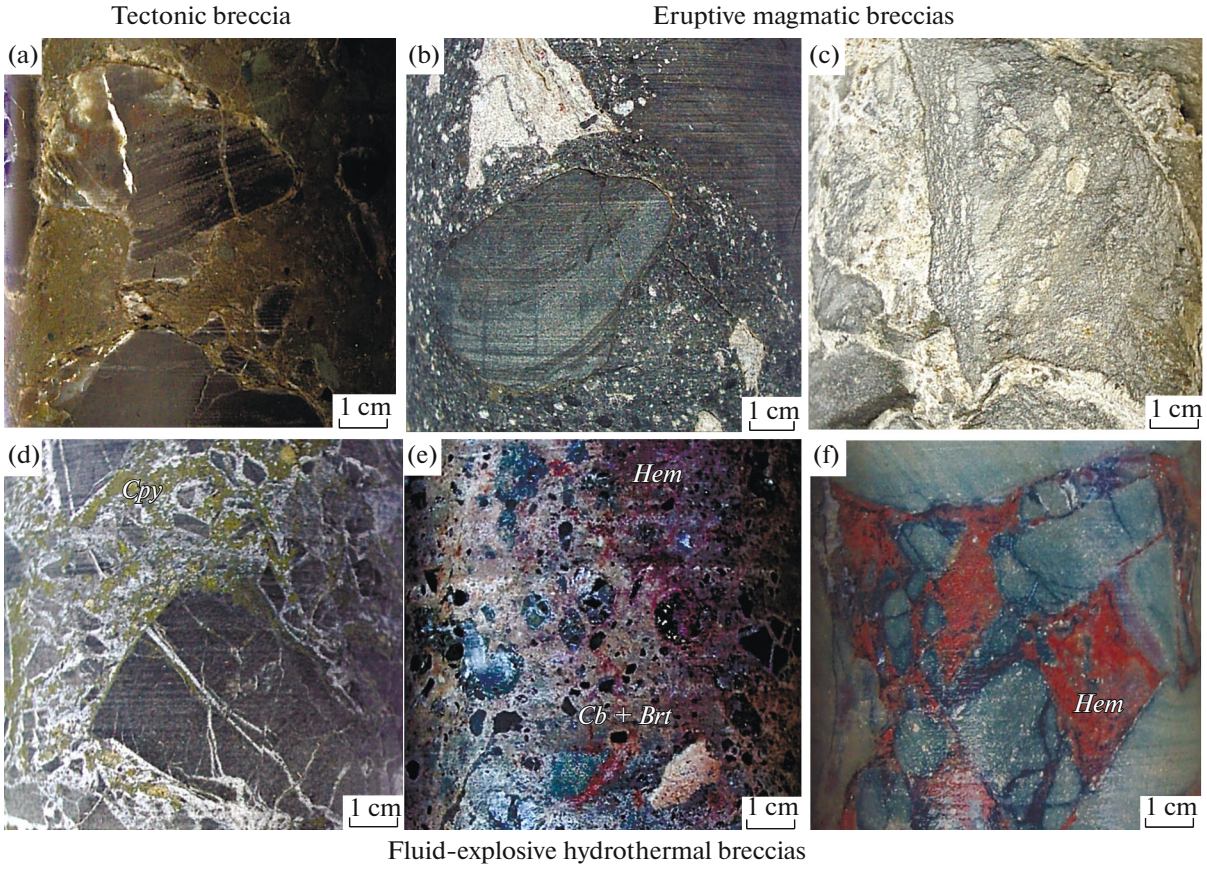

Fig. 5. Different genetic types of breccias widespread within Bezengi ore district and Raduzhnoe deposit. (a) tectonic breccia; (b, c) eruptive magmatic breccias; (d–f) fluid-explosive hydrothermal breccias: (d) silicified mudstone breccia with quartz–barite (*Brt*)-sulfide (*Ccp*+*Py*) cement; (e) mudstone breccia with carbonate(*Cb*)-barite (*Brt*) cement with hematite (*Hem*), reddish color caused by hematite admixture; (f) breccia on argillized rhyolite on hematite (*Hem*) cement.

pyrite, chalcopyrite, galena, sphalerite, quartz, barite, gypsum, and carbonates. Arsenopyrite, bornite, molybdenite, fluorite, and chlorargyrite occur extremely rarely.

Vein and Metasomatic Minerals

The most common nonmetallic mineral at the deposit is *quartz*. The formation of metasomatic quartz, which develops after both sedimentary and igneous rocks, is associated with preore silicification. Quartz of this type forms grains with irregularly serrated outlines. Three varieties of vein quartz are distinguished: (1) gray vein quartz with a granoblastic texture, associated with ore minerals of the Au–sulfide (Figs. 6b, 6c) and polymetallic assemblages (Fig. 7a); (2) chalcedony quartz (Fig. 7b); (3) late white and colorless quartz, forming secant veins, not bearing sulfide mineralization.

Carbonates are represented by Mn-bearing calcite (Fig. 7d), vein (Fig. 7c), and metasomatic (Fig. 7e) dolomite and Fe-dolomite, and less frequently siderite. Based on the SEM-EDS data, calcite and Fe dolomite contain MnO impurities up to 2.04 wt %. Calcite (Fig. 6f) and dolomite, in association with barite, are the main minerals of the Au–Ag low-sulfidation assemblage.

Barite (Fig. 7c) is a typical mineral in the cement of fluid-explosive breccias (Au–Ag low-sulfidation assemblage) and ore veins. According to the SEM-EDS data, it is characterized by an Sr admixture (SrO up to 7 wt %). In fluid-explosive breccias of the Au–Ag low-sulfidation assemblage, barite, together with calcite (Fig. 6a), dolomite, and hematite associates with native gold, chalcopyrite, sphalerite, and acanthite; in veinlets of the polymetallic assemblage (Fig. 6c), with pyrite and sphalerite.

Anhydrite and *gypsum* (Fig. 7d) are widespread at the Raduzhnoe deposit (Pervaya ore zone, Gypsovaya, and Orlinaya zones). As a rule, they occur in shear zones in folded and sheeted mudstones, less frequently in siltstones. These rocks are veined, contain pockets, or are cemented by white, sometimes pinkish white anhydrite-gypsum material. The gypsum forms both single veins and a network of thick veins. The total thickness of gypsiferous strata according to drill-

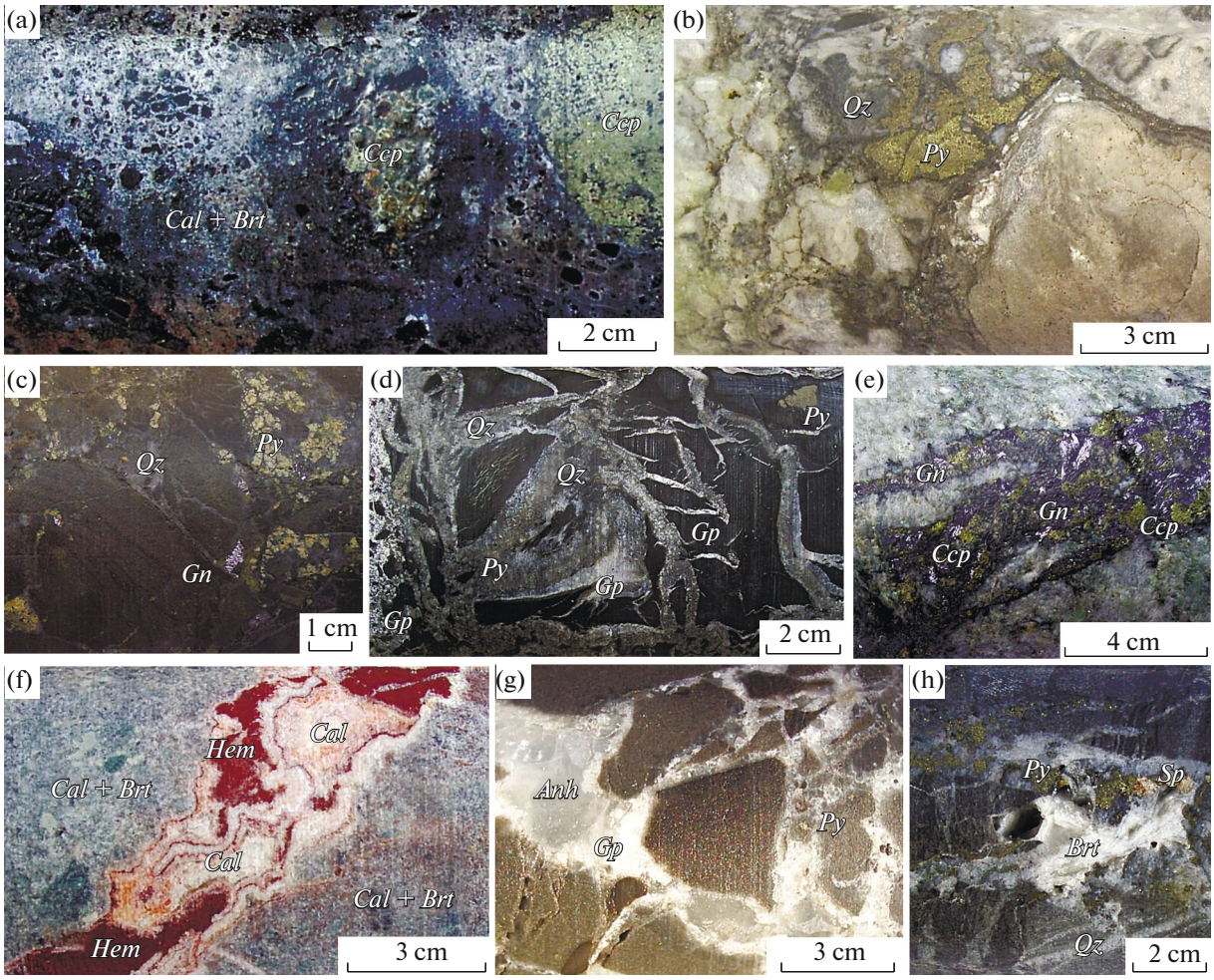

Fig. 6. Structural features of ores and relationship of ore and vein minerals at Raduzhnoe deposit. (a) Mudstone breccias, carbonate–barite cement with chalcopyrite, borehole 3001 (depth interval 69.2–69.4 m); (b) rhyolite breccias with quartz-sulfide cement, borehole 3010 (depth interval 27.5–27.8 m); (c) silicified mudstone breccias with quartz-sulfide cement, borehole 3010 (depth interval 66.5 m); (d) mudstone breccias with quartz–sulfide cement, with gypsum veins, borehole 3016 (depth interval 102–102.2 m); (e) galena–chalcopyrite vein in granites of Belorechensk Complex, borehole 3012 (depth interval 21.6–21.8 m); (f) hematite–carbonate vein in fluid-explosive breccias, shadowy mudstone clasts replaced by barite and carbonate, borehole 3014 (depth interval 45.0 m); (g) silicified mudstone breccias with anhydrite-gypsum cement with pyrite, borehole 3021 (depth interval 111.3–111.4 m); (h) silicified siltstone breccias with quartz-barite-sulfide cement, borehole 3012 (depth interval 17.8–18.6 m).

ing data reaches 65–80 m. The association of gypsum with primary unaltered sulfides (Figs. 6d, 6g), usually the pyrite Au–sulfide assemblage, is characteristic.

Mixed-layered and *clay minerals* are widespread within the deposit. Kaolinite develops after feldspars in sandstones of the Bezengi Formation and basement granites in zones of intensive hydrothermal alteration. Kaolinized rocks are usually very light, almost white in color. Sericite is found in altered basement granites and sandstones of the Bezengi Formation. The minerals of the illite–smectite group are widespread in volcanic rocks of the Khulam Complex, where, as a result of low-temperature argillization, they replace both bulk rocks (Fig. 7f) and K-feldspar phenocrysts. Montmorillonite forms fine fibrous aggregates, developing after plagioclase and glass residues in argillized rhyolite. Celadonite develops in contact zones between rhyolite and trachyte bodies and host mudstones, often giving the rocks an emerald green color.

Ore Minerals

Pyrite is present in almost all mineral assemblages of the Raduzhnoe deposit and is very diverse in shape and size, which probably indicates that it belongs to several generations. Conditionally, based on the morphology of pyrite segregations and the features of its composition and occurrence, four generations of pyrite have been identified (Fig. 8).

Pyrite-I (sedimentary-diagenetic) forms layer-by-layer or disperse disseminations in Jurassic sedimentary rocks (Fig. 8a). It is represented by framboids and

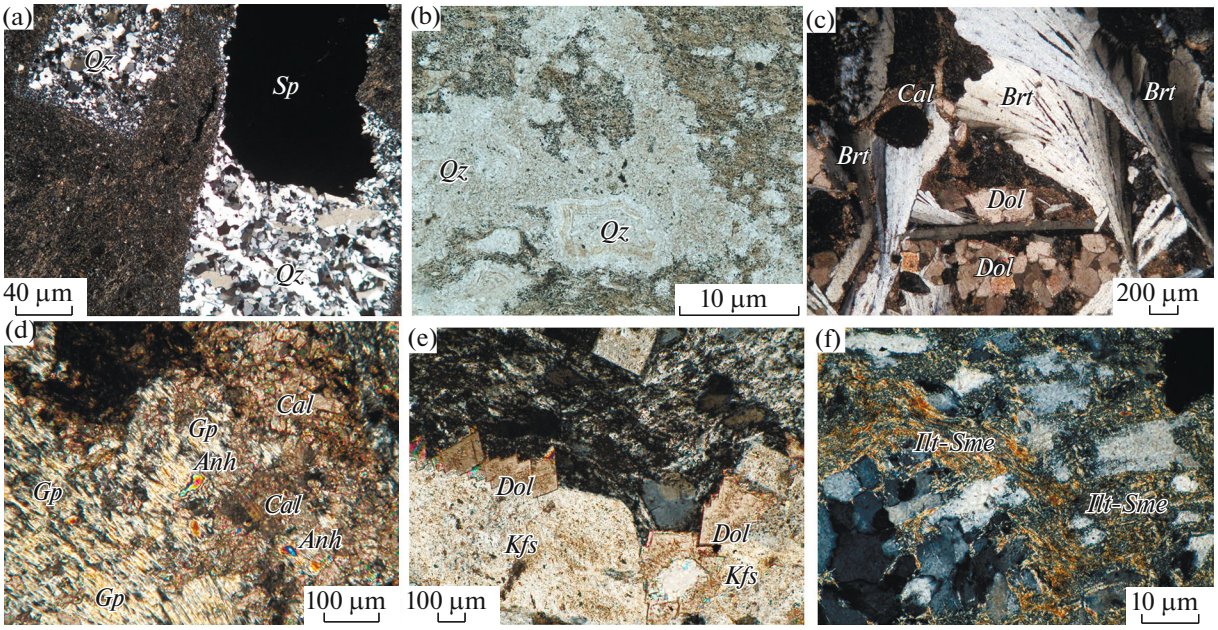

Fig. 7. Vein and metasomatic minerals of Raduzhnoe deposit. (a) sphalerite (*Sp*)-quartz (*Qz*) veinlets in breccias on silicified siltstones, Lagernaya Zone, sample R-22, crossed nicols ; (b) chalcedony quartz (*Qz*) in cement of brecciated argillized rhyolites; Orlinaya Zone, sample R-3/2-181, parallel nicols ; (c) sheaf-shaped barite crystals (*Brt*) in dolomite (*Dol*)-calcite (*Cal*) groundmass, sample 3009/15; (d) anhydrite (*Anh*) and gypsum (*Gp*) with later superimposed calcite (*Cal*), Pervaya ore zone, sample 3001/6, crossed nicols ; (e) superimposed dolomite (*Dol*) replacing Kfs phenocrysts (*Kfs*) in rhyolites, Orlinaya ore zone, sample R-3/2-181, crossed nicols ; (f) mixed-layered illite-smectites (*Ilt-Sme*), developed after groundmass of argillized rhyolites, sample R-6, crossed nicols.

small cubic crystals up to 20 μm in size. Pyrite-I is characterized by an extremely low Cu content (0.2 wt %), with impurities of As 0.06–2.16 wt %, Sb 0.05–0.23 wt %, Ni 0.11–0.16 wt %, and Co 0.06–0.11 wt %.

Pyrite-II occurs in sericitized and propylitized granites, sedimentary rocks, and volcanic rocks of Jurassic age. It is characterized by crystals with a pentagonal-dodecahedron shape up to 200 μm in size (Fig. 8b). The disperse disseminations of pyrite-II phenocrysts are associated with sericite, chlorite, and anatase. Zonal distribution of As impurity (0.46–2.17 wt %) in different zones of growth of a single crystal was established in pyrite-II. Insignificant admixtures of Cu (0.10–0.26 wt %), Sb (0.06–0.07 wt %), and Co (0.06–0.07 wt %) are also noted.

Pyrite-I and pyrite-II are considered preore minerals.

Pyrite-III is the main mineral of the Au–sulfide assemblage, which usually forms hypidiomorphic segregations in association with sphalerite, chalcopyrite, fahlore, and galena in sulfide and quartz–sulfide ores (Fig. 8c). This morphological type of pyrite is characterized by the following impurities (wt %): As 0.06–0.19, Cu 0.06–1.25, Co 0.06–0.07, and Ni 0.06–0.09; no Sb impurity has been found.

Pyrite-IV forms euhedral crystalline segregations in quartz–sulfide cement and veinlets in fluid-explosive breccias (Fig. 8d). This type of pyrite forms close

Table 2. Mineral composition of ore asscoaitons of Raduzhnoe deposit

Assocaitions	Au–Ag low-sulfidation assemblage	Au–sulfide assemblage	Polymetallic assemblage
Main minerals	Acanthite, sphalerite, galena, hematite, barite, calcite, dolomite, ***Fe-dolomite***	Pyrite, chalcopyrite, sphalerite, galena, fahlore **(*tetrahedrite*-(*Zn*), *tennantite*-(*Fe*,*Zn*)), bournonite**, quartz, gypsum, anhydrite	Quartz, chalcopyrite, sphalerite, galena
Rare minerals	Native gold	Native gold, barite, calcite, dolomite	Pyrite

Minerals, first discovered by authors in ores of Raduzhnoe deposit are shown in italic.

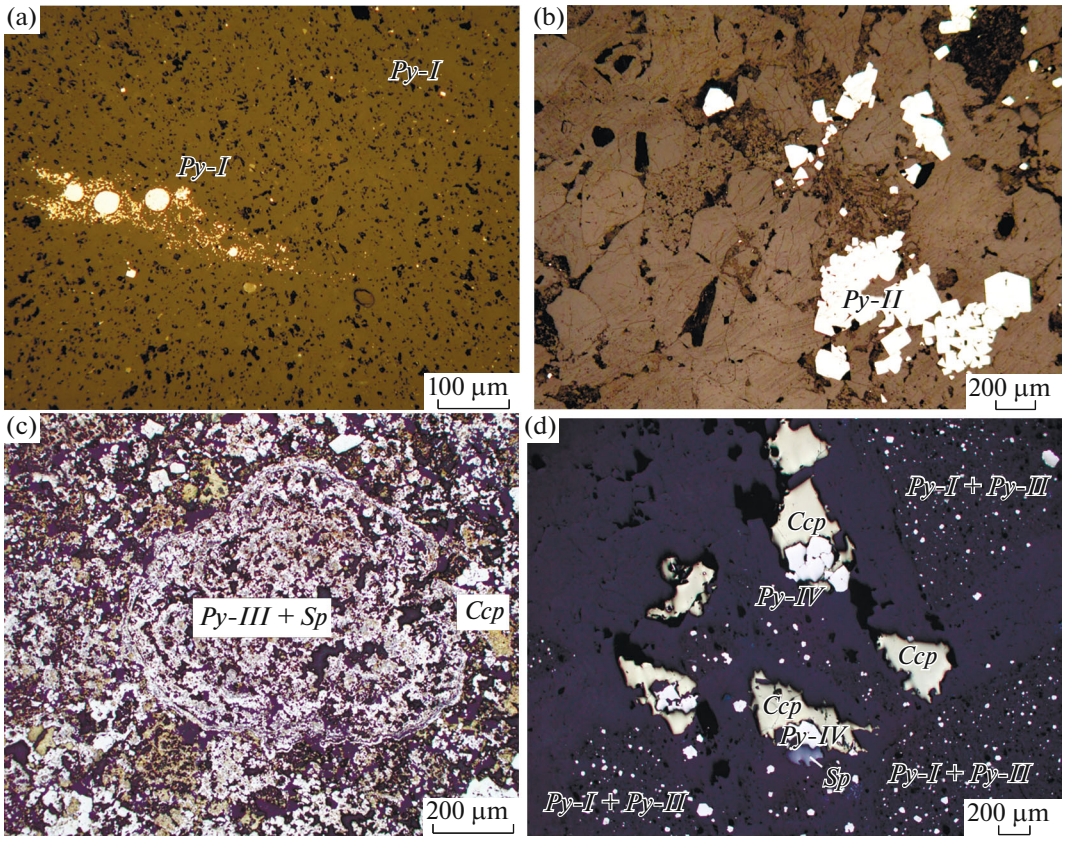

Fig. 8. Pyrite of different generations on polished thin sections. (a) pyrite-I and pyrite-II, sample R-18; (b) pyrite-II in silicified argillized sandstones of Bezengi Formation, sample 3/2-210; (c) intergrowths of globular pyrite-III with chalcopyrite (*Ccp*), sphalerite (*Sp*) and galena from sulfide ores, Pervaya ore zone, sample 3001/4; (d) pyrite-IV in fluid-explosive breccias after siltstones, siltstone fragments are silicified; there is also fine impregnation of pyrite-I and pyrite-II, sulfide-quartz cement of breccias includes chalcopyrite (*Ccp*) and sphalerite (*Sp*), sample R-17.

intergrowths with quartz, barite, sphalerite, chalcopyrite, and galena. Pyrite-IV is characterized by impurities of As 0.23–3.55 wt %, Cu 0.13–0.42 wt % and minor impurities of Co (0.08 wt %), Ni (0.09 wt %), and Sb (0.10–0.20 wt %).

Sphalerite forms intergrowths with galena, chalcopyrite, and pyrite as irregularly shaped aggregates (Figs. 8d, 10c, 10f, 11c, 11f).

Sphalerite of the Raduzhnoe deposit is characterized by a low Fe content (≤0.22 wt % Fe) and is classified as cleiophane. The composition of sphalerite from different assemblages was measured by EPMA (35 analyses). According to the data obtained, Au–sulfide and Au–Ag low-sulfidation assemblages include two types of sphalerite, which vary insignificantly in composition.

Sphalerite-I associates with pyrite, chalcopyrite, and galena in sulfide ores and quartz–sulfide veins. The composition of sphalerite-I (wt %) is Zn 59.19–66.58, S 31.26–33.29. Sphalerite-I contains the following impurities (wt %): Fe 0.11–0.98; Cd 0.11–1.04; Cu 0.05–0.36, In 0.09–0.11, and Hg 0.06.

Sphalerite-II most often associates with barite and carbonates (dolomite, calcite). Grains of this type of sphalerite are often covered by a thin acanthite film. The composition of sphalerite-II (wt %) is Zn 63.31–67.31, S 32.43–33.21. Sphalerite-II contains the following impurities (wt %): Fe 0.01–0.05, Cd 0.24–0.62, In 0.07–0.09, Sn 0.04–0.05, Cu 0.06.

Sphalerite of the Au–Ag low-sulfidation assemblage is characterized by minimum Fe contents (less 0.1 mol % FeS) compared to sphalerite of the Au–sulfide assemblage (0.2–1.1 mol % FeS). As well, the Cd contents in both assemblages fall into almost the same range of 0.1–0.6 mol % CdS (Fig. 9a), while there are single analyses of sphalerite from the Au–sulfide assemblage where the Cd content reaches 0.8–1.0 mol % CdS).

Galena occurs both as single crystals and aggregates of grains, as well as forming intergrowths with chalcopyrite. Crystals are usually from tenths of to 1–3 mm; in fluid-explosive breccia cement, from a few microns to 0.1 mm; in monomineralic segregations, from crystals up to 2 cm across. In the Au–sulfide assemblage, galena occurs together with sphalerite, pyrite, and chalcopyrite (Fig. 8c). An EPMA study of galena

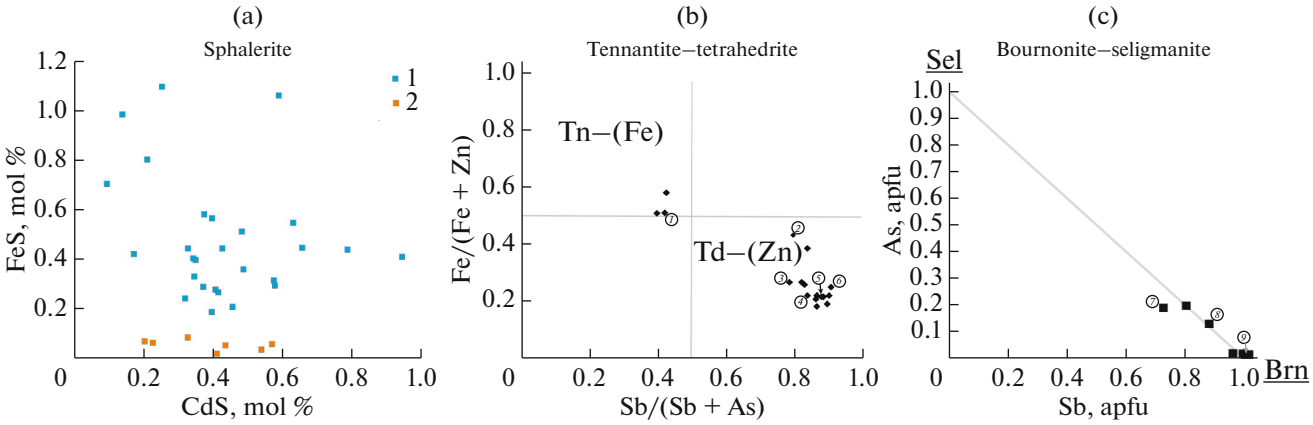

Fig. 9. Ratios of some isomorphic elements in solid solutions of Raduzhnoe deposit. (a) CdS–FeS ratio (mol %) in sphalerite from gold-sulfide (1) and gold–silver low-sulfidation assemblages (2). (b) Sb/(Sb+As)–Fe/(Fe+Zn) ratio in fahlore. (c) Sb–As ratio (apfu) in bournonite. Numbers in circles (1–9) correspond to analyses presented in Table 3.

showed that its composition is stoichiometric and in most cases the contents of impurity elements (Cd, As, Se) are below the detection limit. Based on 48 analyses, only a few samples showed the presence of impurities (wt %): Ag 0.07, Sb 0.13, Bi 0.09–0.13, Cu 0.19–0.60, and Fe 0.06–3.77.

Chalcopyrite is found at all ore zones of the Raduzhnoe deposit. It forms intergrowths with sphalerite and galena, surrounds pyrite and galena crystals, and fills interstitial spaces in cataclased pyrite and sphalerite. It is also associated with native gold, together with sphalerite, galena, and fahlore.

Sulfosalts at the deposit, represented mainly by *fahlore* and, rarely, *bournonite*, were found in almost all ore zones. They occur in minor amounts as sporadic segregations in association with chalcopyrite, sphalerite, galena, and pyrite (Fig. 10). Their content in ores does not exceed 1 vol %. EPMA was used to study sulfosalts for the first time in sulfide ore samples from the Orlinaya and Kishlyk-su zones.

Fahlore occurs in intergrowths with sphalerite, galena, chalcopyrite, and bournonite, as well as in pyrite as small isometric inclusions (Fig. 10).

Based on 17 analyses, the contents of rock-forming elements in fahlore are as follows (wt %): Cu 33.64–39.47, Ag 0.39–3.56, Zn 4.09–6.83, Fe 1.26–4.81, Pb up to 0.13, Cd up to 0.17, Sb 12.39–27.64, As 1.77–11.57, Bi up to 0.17, S 25.52–27.95, Se up to 0.11 (Table 3, analyses 1–6). The Sb/(Sb + As) and Fe/(Fe + Zn) ratios are 0.40–0.91 and 0.58–0.18, respectively. The fahlore demonstrates an inverse correlation between the Sb/(Sb + As) and Fe/(Fe + Zn) ratios (Fig. 9b). According to the recent notation (Biagioni et al., 2020), fahlore at the Raduzhnoe deposit is represented mainly by Ag-bearing tetrahedrite-(Zn), and rarely by Ag-bearing tennantite-(Fe) and tennantite-(Fe,Zn). Based on X-ray data, fahlore was previously classified as Ag-bearing tetrahedrite (Koptyukh et al., 1985(ar); Kryazhev and Dvurechenskaya, 2014(ar)).

Bournonite was found at the deposit, and described by the authors for the first time. It occurs as xenomorphic segregations in galena and tetrahedrite (Figs. 10d–10e). Probably, bournonite replaces the latter, since there are chains of its tiny segregations in galena (Fig. 10e) and thin and short veinlets—in tetrahedrite (Fig. 10d). Based on EPMA data (8 analyses), the contents of elements in bournonite are as follows (wt %): Pb 39.87–46.79, Cu 11.47–14.21, Sb 17.90–26.09, As 0.29–3.10, S 19.74–20.24, Zn 0.43–1.84, Fe 0.23–0.82; Ag, Hg, Cd, Bi, Se are below the limit of detection (Table 3, analyses 7–9). Thus, at the Raduzhnoe deposit, the bournonite–seligmanite solid solution with continuous isomorphism in the Sb/(Sb + As) interval from 0.98 to 0.79 was found (Fig. 9c).

We attempted to apply ore geothermometry to sulfide solid solutions from the Raduzhnoe deposit. Fahlore (tetrahedrite) and sphalerite have smooth mutual boundaries and show no signs of corrosion (Figs. 10a, 10f), which may evidence the paragenesis of these minerals. The composition of sphalerite, coexisting with tetrahedrite (Table 3, analysis 3) is as follows (wt %): Zn, 61.64; Fe, 0.57; S, 37.79; 0.96 mol % FeS. The temperature calculated for this pair of minerals as per the geothermometer (Sack and Loucks, 1985) is estimated at 162 ± 25°C. The crystallization temperature of sphalerite–tetrahedrite paragenesis does not contradict the crystallization conditions of these minerals, and this is why it could be considered reliable and characterizes the crystallization conditions of this mineral assemblage at the deposit.

No relationships between fahlore and bournonite in ores were established. The bournonite inclusions in tetrahedrite may indicate either simultaneous formation of these minerals (tapping of bournonite grains during crystallization of tetrahedrite) or later formation of bournonite with respect to tetrahedrite

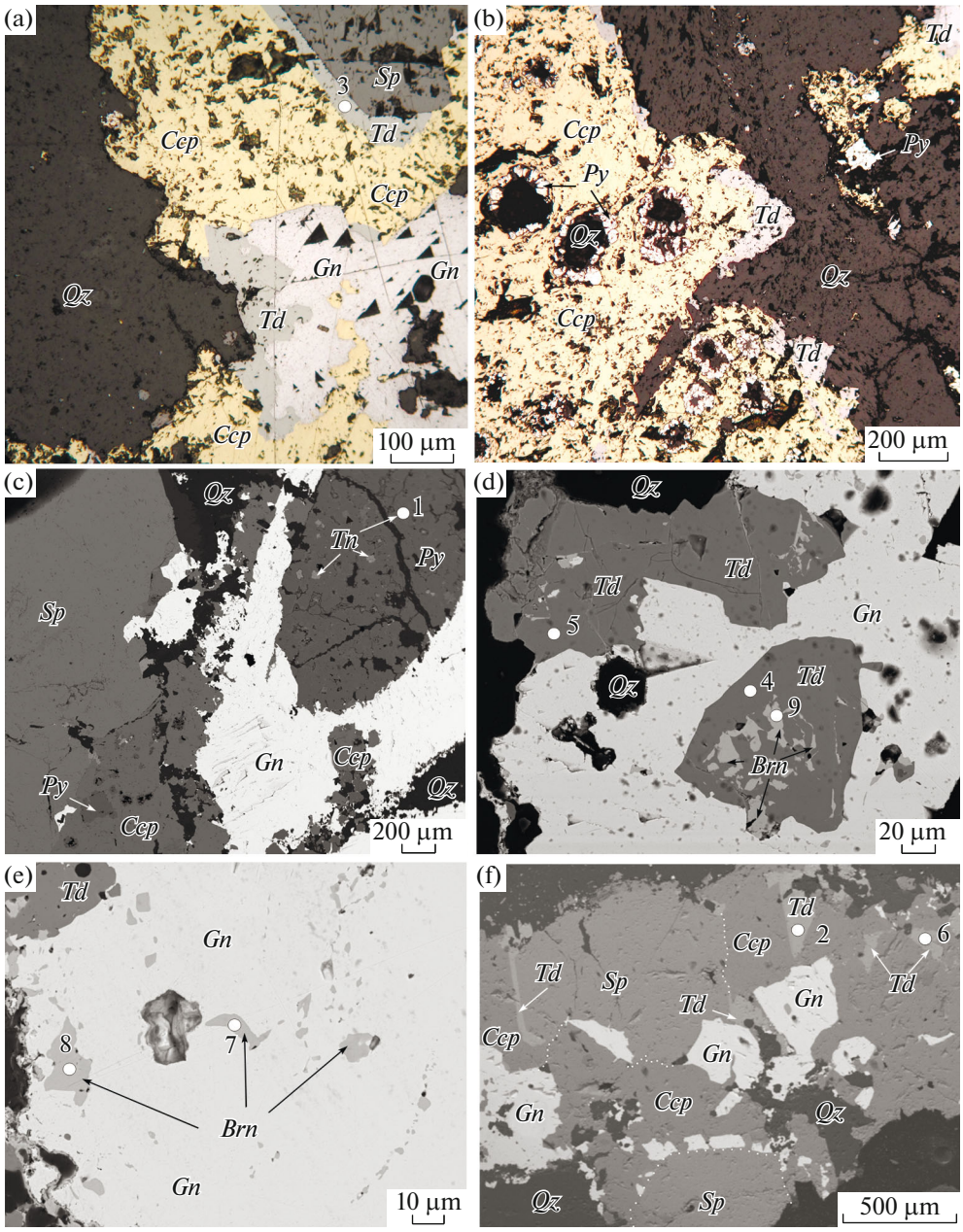

Fig. 10. Relationship of sulfosalts with other minerals in sulfide of ore zones Orlinaya and Kishlyk-su. (a) Intergrowths of sphalerite (*Sp*), tetrahedrite (*Td*), galena (*Gn*), and chalcopyrite (*Ccp*). Tetrahedrite overgrows sphalerite and forms intergrowths with galena. Chalcopyrite fills interstitial space between grains of these minerals, replacing sphalerite and galena and develops along fractures; (b) intergrowths of chalcopyrite, tetrahedrite, and pyrite (*Py*). Tetrahedrite develops along contact between chalcopyrite and quartz (*Qz*) grains. Chalcopyrite grains include ring segregations, composed of small pyrite grains along rim and quartz in central part; (c) intergrowth of sphalerite, pyrite, galena, and chalcopyrite. Pyrite contains small isometric inclusions of tennantite (*Tn*); (d) intergrowth of galena and tetrahedrite, including xenomorphic secretions of bournonite (*Brn*); (e) xenomorphic inclusions of bournonite and chains of small rounded inclusions in galena; (f intergrowth of sphalerite, chalcopyrite, galena and fahlore. Fahlore and galena develop along contact between sphalerite and chalcopyrite. Numbers of composition points in Fig. 10 correspond to numbers of analyses in Table 3. Sample A-2/2-187 (a, b, c, f) and KS-2/4 (d, e). Reflected light images (a–b) and BSE images (c–f).

(replacement of tetrahedrite by bournonite in small pores and cracks). The formation temperature of bournonite–fahlore assemblages calculated with the geothermometer (Sack and Ebel, 1993) is unrealistic. This indicates that equilibrium between these solid solutions was not reached or was violated; it confirms the hypothesis of a later deposition of bournonite.

Hematite forms finely dispersed masses in the cement of fluid-explosive breccias, occurring both in the oxidation zone of the deposit and its deep horizons (Figs. 5d, 6f).

Table 3. EPMA and SEM-EDS analyses of fahlore and bournonite from Raduzhnoe deposit

Analysis no.	Mineral	Ag	Cu	Zn	Fe	Pb	Sb	As	Bi	S	Total	Sb/(Sb + As)	Fe/(Fe + Zn)
1	Tn-(Fe,Zn)	1.29	39.47	4.49	3.99	n.d.	12.89	10.94	0.07	27.88	101.09	0.420	0.509
		$(Cu_{9.50}Ag_{0.18})_{\Sigma 9.69}(Zn_{1.05}Fe_{1.09})_{\Sigma 2.14}(Sb_{1.62}As_{2.23})_{\Sigma 3.85}S_{13.30}$											
2	Td-(Zn)	3.35	35.55	4.52	2.95	n.d.	23.69	3.73	n.d.	26.21	100.00	0.796	0.433
		$(Cu_{9.14}Ag_{0.51})_{\Sigma 9.65}(Zn_{1.13}Fe_{0.86})_{\Sigma 1.99}(Sb_{3.18}As_{0.81})_{\Sigma 3.99}S_{13.36}$											
3		3.11	34.34	5.50	1.70	n.d.	24.02	4.06	n.d.	27.29	100.02	0.785	0.266
		$(Cu_{8.77}Ag_{0.47})_{\Sigma 9.24}(Zn_{1.37}Fe_{0.49})_{\Sigma 1.86}(Sb_{3.20}As_{0.88})_{\Sigma 4.08}S_{13.82}$											
4		0.44	37.76	6.01	1.45	0.06	24.96	2.96	0.12	25.80	99.61	0.838	0.220
		$(Cu_{9.75}Ag_{0.07})_{\Sigma 9.82}(Zn_{1.51}Fe_{0.43})_{\Sigma 1.93}(Sb_{3.36}As_{0.65})_{\Sigma 4.01}S_{13.21}$											
5		0.41	38.08	6.12	1.45	0.07	25.05	2.10	0.16	26.13	99.63	0.880	0.217
		$(Cu_{9.80}Ag_{0.06})_{\Sigma 9.86}(Zn_{1.53}Fe_{0.42})_{\Sigma 1.95}(Sb_{3.37}As_{0.46})_{\Sigma 3.82}S_{13.33}$											
6		2.95	33.92	5.52	1.55	n.d.	27.64	1.77	n.d.	26.64	99.99	0.906	0.247
		$(Cu_{8.82}Ag_{0.45})_{\Sigma 9.27}(Zn_{1.40}Fe_{0.46})_{\Sigma 1.86}(Sb_{3.75}As_{0.39})_{\Sigma 4.14}S_{13.73}$											
7	Brn	n.d.	11.71	0.06	0.16	46.79	17.90	2.92	n.d.	19.74	99.39	0.791	
		$Pb_{1.11}Cu_{0.91}(Sb_{0.73}As_{0.19})_{\Sigma 0.92}S_{3.04}$											
8		n.d.	12.73	0.07	n.d.	41.01	22.20	2.02	n.d.	20.24	98.44	0.871	
		$Pb_{0.96}Cu_{0.97}(Sb_{0.88}As_{0.13})_{\Sigma 1.01}S_{3.05}$											
9		n.d.	14.16	0.38	n.d.	40.16	25.79	0.29	n.d.	20.02	100.90	0.982	
		$Pb_{0.92}Cu_{1.06}(Sb_{1.01}As_{0.02})_{\Sigma 1.03}S_{2.96}$											

Tn-(Fe,Zn)—tennantite-(Fe,Zn); Td-(Zn)—tetrahedrite-(Zn); Brn—bournonite-seligmanite; n.d., not determined. Analyses 2, 3, and 6 were performed on a scanning electron microscope; other analyses, on an electron microanalyzer. The table shows analyses of a representative set of samples, the numbers of which correspond to those in Fig. 9. The composition points of all analyzed samples are shown in Figs. 9b, 9c.

Mineral phases of Au and Ag at the Raduzhnoe deposit are represented by low fineness native gold and silver, acanthite, and chlorargyrite. Chlorargyrite is a rare hypergene mineral, which developed after acanthite.

Acanthite is the main Ag-bearing mineral of the Au–Ag low-sulfidation assemblage, which occurs in fluid-explosive breccias together with sphalerite, galena, carbonates, and barite. The content of acanthite in fluid-explosive breccias varies from fractions to 5 vol %.

Native gold occurs mainly in chalcopyrite and galena (Fig. 11), forming irregularly shaped segregations 5–15 μm in size; the fineness is low (419–670‰ based on ten microprobe analyses). Hg impurities are noted in gold, up to 4.6 wt % (Table 4). The composition of the solid solution of the Au–Ag–Hg system at the Raduzhnoe deposit can be represented by the formula $(Au_{0.571–0.791}Ag_{0.207–0.390}Hg_{0.002–0.062})$ for Au 41.91–67.02, Ag 32.05–51.98, and Hg 0.15–4.64 wt %. The solid solutions of this system and thermodynamic conditions of their formation are considered in detail in (Chudnenko and Palyanova, 2016). Due to a relatively low Hg content in native gold of the Raduzhnoe deposit, it can not be attributed to Hg-bearing gold. As known from (Naumov, 2007), subsurface deposits, where the processes of boiling solutions are widely manifested, are characterized by low-Hg gold.

Native silver (one analysis, Table 4) was established, according to the data from (Koptyukh et al., 1985(ar)), in ores of the Au–Ag low-sulfidation assemblage of the Pervaya Ore Zone. The occurrence of native silver in ores (the formula of the solid solution can be represented as $Au_{0.285}Ag_{0.566}Hg_{0.149}$), bearing 19.32 wt % Au and 9.93 wt % Hg, needs additional study since its presence can indicate both the change in thermodynamic conditions of ore genesis at the latest stages of ore genesis and the development of exogenic processes.

Hypergene Minerals

In the oxidation zone of the deposit, which is a few meters thick, minerals of the alunite supergroup, malachite, azurite, chalcocite, limonite, jarosite, cerussite, and anglesite were found. Secondary Pb minerals are represented by cerussite, anglesite, and pyromorphite developed after galena. Minerals of the alunite supergroup occurring mainly in the thin oxidation zone were first described at the Raduzhnoe deposit. Plumbojarosite occurs in the oxidation zone of the exposed orebodies. Minerals of the plumbojarosite–

Table 4. Compositions of native gold and silver from Raduzhnoe deposit, EPMA data (wt %)

Ser. no	Sample no.	Au	Ag	Hg	Cu	Fe	Total	Fineness of gold, ‰
1	3001-2-1	41.91	51.98	2.62	0.00	0.00	96.51	419
2	3001-2-2	43.27	50.76	4.64	0.00	0.00	98.67	434
3	3001/4-1	64.57	32.56	0.00	0.00	0.00	97.13	646
4	3001/4-2	67.02	32.08	0.00	0.00	0.00	99.10	670
5	3001/4-3	65.30	32.05	0.00	0.00	0.00	97.34	653
6	3001/4-4	61.94	34.96	0.91	0.00	0.00	97.80	619
7	3001/4-5	65.35	32.29	0.00	0.00	0.00	97.64	653
8	3001/4-12	50.21	47.79	0.00	0.00	0.00	98.00	502
9	3001/5-6	50.03	43.98	0.00	0.72	0.41	95.15	500
10	3001/5-7	57.15	38.21	0.00	0.29	0.31	95.97	571
11	Data from (Koptyukh et al., 1985(ar))	19.32	70.12	9.93	0.00	0.00	99.37	193

kintoreite series form crusts and loose masses, filling cavities of dissolution of sulfides in the quartz cement of the fluid-explosive breccias together with limonite, rarely intergrowths of rhombohedral crystals. The high-altitude conditions, combined with an arid climate and exposure of sulfide orebodies at the surface, contributed to a high evaporation rate and a decrease in pH, which led to the formation of minerals of the alunite supergroup in a relatively thin sulfide ore oxidation zone. The studied minerals contain Pb (14.84–33.46 wt % PbO), Cu (0.13–2.27 wt % CuO), and As (0.0–7.68 wt % As_2O_5). According to this, they can be attributed to the plumbojarosite–beudantite and plumbojarosite–kintoreite series. Essential admixtures of Cu, Pb, As in minerals of the alunite supergroup in the oxidation zone of the Raduzhnoe deposit indicate that they formed as a result of oxidation of sulfide ores and can not be considered endogenic minerals, formed synchronously with the ore deposition. The absence of these minerals in the exocontact zone of non-oxidized segments of orebodies testifies in favor of the hypergene origin of alunite and jarosite.

RESULTS OF STUDYING THE Pb ISOTOPIC COMPOSITION IN ORES AND HOST ROCKS OF THE RADUZHNOE DEPOSIT

Pb Isotopic composition of Ores of the Raduzhnoe Deposit

The Pb isotopic data were obtained for 10 galena samples that were collected from all mineral assemblages of the Raduzhnoe deposit described above. The measured Pb isotopic ratios vary in the following ranges: for $^{206}Pb/^{204}Pb$, 18.205–18.360; $^{207}Pb/^{204}Pb$, 15.593–15.665; and $^{208}Pb/^{204}Pb$, 38.466–38.599 (Table 5). In total, the revealed variations in the Pb isotopic composition at the deposit are small-scale. The maximum variation coefficient ($\nu_{6/4} = 0.24\%$) was obtained for the $^{206}Pb/^{204}Pb$ ratio, whereas for the $^{207}Pb/^{204}Pb$ and $^{208}Pb/^{204}Pb$ ratios, they were almost two times lower ($\nu_{7/4} = 0.14\%$ and $\nu_{8/4} = 0.13\%$) and close to each other. There is no correlation between Pb isotopic composition in the sample and its sampling site on the one hand or its belonging to the mineral assemblage, on the other. Thus, the Raduzhnoe deposit is characterized by a sufficiently homogeneous Pb isotopic composition. Such a feature is usually typical of gold-bearing ore-forming systems, genetically associated with magmatism (Chugaev et al., 2013b, 2021; Lebedev et al., 2016, 2018; Chernyshev et al., 2018).

Pb Isotopic composition of Host Rocks

The Pb isotopic composition was studied in igneous and sedimentary rocks, which are widespread in the area of the Raduzhnoe deposit. They are represented by Middle Jurassic subvolcanic rocks of different composition of the Khulam Complex (four samples) and black shales (four samples). The Pb, Th, and U contents, as well as the Pb isotopic composition, were measured in bulk samples (Table 6).

The Pb, Th, and U contents in the studied rocks vary in a wide range (ppm): from 2.6 to 25.5, from 1 to 13, and from 0.25 to 2.6, respectively. The samples are characterized by high $^{238}U/^{204}Pb$ and $^{232}Th/^{204}Pb$ ratios, which range from 2.3 to 42 and from 9.3 to 253. The minimum $^{238}U/^{204}Pb$ and $^{232}Th/^{204}Pb$ ratios were obtained for gabbroids of the Khulam Complex (sample R-19), and the maximum, for black shales. Because of such high and greatly variable $^{238}U/^{204}Pb$ and $^{232}Th/^{204}Pb$ ratios, correction of $^{206}Pb/^{204}Pb$ and $^{208}Pb/^{204}Pb$ ratios to an age of 167 Ma (U–Pb age of

Table 5. Pb isotopic composition in galena from Raduzhnoe gold-ore deposit (MC-ICP-MS) and model parameters of Pb source according to Stacey–Kramers model (Stacey and Kramers, 1975)

Ser no.	Sample no.	$^{206}Pb/^{204}Pb$	$^{207}Pb/^{204}Pb$	$^{208}Pb/^{204}Pb$	μ_2	Tm	ω_2	Th/U
1	R-17	18.2879	15.6574	38.5512	9.96	370	40.1	4.03
2	3001/7	18.3589	15.6622	38.5922	9.97	327	39.9	4.00
3	Kh-2	18.2050	15.5928	38.4663	9.70	302	38.9	4.01
4	2/3-187	18.3601	15.6648	38.5988	9.98	332	40.0	4.01
5	RTs-7	18.2812	15.6485	38.5067	9.93	357	39.7	4.00
6	3001/12	18.2944	15.6628	38.5834	9.99	376	40.4	4.04
7	RTs-3	18.2883	15.6525	38.5203	9.94	360	39.9	4.01
8	3/2-181	18.2633	15.6453	38.5096	9.92	364	39.8	4.02
9	R-12	18.2794	15.6449	38.4915	9.91	351	39.6	4.00
10	R-23	18.2894	15.6635	38.5929	9.99	381	40.5	4.05

Measurement error of Pb isotope ratio in galena did not exceed ±0.02% (2SD).

rocks of the Khulam Complex (Kaigorodova and Lebedev, 2022)) was significant, reaching 6.4% for $^{206}Pb/^{204}Pb$ and 4.5% for $^{208}Pb/^{204}Pb$. Overall, the age-corrected Pb isotopic ratios fall within relatively narrow ranges. In Jurassic volcanic rocks of the Khulam Complex, $^{206}Pb/^{204}Pb$ = 18.06–18.37, $^{207}Pb/^{204}Pb$ = 15.60–15.64 and $^{208}Pb/^{204}Pb$ = 38.00–38.32; in black shales, $^{206}Pb/^{204}Pb$ = 18.23–18.40, $^{207}Pb/^{204}Pb$ = 15.61–15.63, and $^{208}Pb/^{204}Pb$ = 37.96–38.344 (Table 6).

Figure 12 shows the comparison of the Pb isotopic data obtained for galena from the Raduzhnoe deposit, as well as the age-corrected Pb isotopic compositions of the Jurassic volcanic rocks and black shales. In addition, the diagrams show the evolution curves of the Pb isotopic composition in the Earth's global reservoirs, namely, "upper crust" and "orogen," according to the Zartman–Doe model (Zartman and Doe, 1981) and Stacey–Kramers model (Stacey and Kramers, 1975).

In the $^{206}Pb/^{204}Pb$–$^{207}Pb/^{204}Pb$ diagram (Fig. 12a), most points of galena fit significantly higher than the Stacey–Kramers average crustal growth curve and near the curve describing the evolution of Pb isotopic composition in the upper crustal geochemical reservoir. This indicates a high U/Pb ratio at the source of ore lead. The only exception is a point of sample X-2 (galena from trachytes of the Khulam Complex), which is below the main group near the "orogen" curve. The data points of galena, which have a large scatter (MSWD = 75), yield a subvertical trend, reflecting a positive correlation (r = 0.82) between $^{206}Pb/^{204}Pb$ and $^{207}Pb/^{204}Pb$ ratios. In turn, the data points of Jurassic rocks form two independent fields near the middle crustal evolution curve. One of them is formed by the data points of volcanic rocks of the Khulam Complex, some of which fall on the trend of the Pb isotopic composition of galena. The second field, corresponding to the black shales, is shifted to the right with respect to the curves of both the ore lead and lead in volcanic rocks.

In the $^{206}Pb/^{204}Pb$–$^{208}Pb/^{204}Pb$ diagram, data points of galena fit between average crustal growth curve (ω_2 = 36.84) and the Stacey-Kramers model curve with ω_2 = 42. This is evidence of higher Th/Pb and Th/U ratios in a source of ore lead (Fig. 12b). As in the diagram with radiogenic isotopes ^{206}Pb and ^{207}Pb, data points of galena are widely spread along the linear trend (MSWD = 66). The correlation coefficient between $^{206}Pb/^{204}Pb$ and $^{208}Pb/^{204}Pb$ ratios is 0.81. The fields of volcanic rocks of the Khulam Complex and black shales lie somewhat lower than the trend being confined to the average crustal growth curve. At this, the field of volcanic rocks fits on the lower continuation of the ore lead curve.

DISCUSSION

Age of the Raduzhnoe Deposit

In the course of our research, we did no direct dating of ore-bearing metasomatic formations of the Raduzhnoe Au–sulfide deposit. However, a conclusion about its age can be made based on the correlation of previous isotope-geochronological data and the published results of geological and stratigraphic investigations within this region.

Our recent U–Pb dating (Kaigorodova and Lebedev, 2022) of the moderately felsic and felsic volcanic rocks of the Khulam Complex, widespread in the Bezengi ore district, allowed us to establish that they were erupted from the Bajocian to the Callovian (167 ± 3 Ma). Note that the intrusions of the Khulam Complex everywhere cut through the Bajocian terrigenous rocks but they are not observed in the Callovian strata, which are also present within the deposit area. During the Bathonian, the region was uplifted above sea level, and sedimentary deposits of this time were absent

Table 6. Pb–Pb isotopic data, U, Th and Pb contents in bulk samples of Jurassic igneous rocks of Khulam Complex and black shales of Raduzhnoe deposit

Ser. no.	Sample no./ characteristics	Pb, ppm	Th, ppm	U, ppm	Measured			Corrected for 167 Ma		
					$^{206}Pb/^{204}Pb$	$^{207}Pb/^{204}Pb$	$^{208}Pb/^{204}Pb$	$(^{206}Pb/^{204}Pb)_t$	$(^{207}Pb/^{204}Pb)_t$	$(^{208}Pb/^{204}Pb)_t$
1	210-1/13/rhyolite	7.19	12.31	2.04	18.6258	15.6612	39.2104	18.373	15.638	38.241
2	210-2/13/ same	5.14	6.40	0.88	18.3497	15.6124	38.6796	18.143	15.637	38.265
3	210-5/13/tra-chyandesibasalt	2.63	1.01	0.30	18.4481	15.6131	38.5242	18.062	15.598	38.000
4	R-19/gabbro	6.80	0.97	0.25	18.2868	15.6076	38.3898	18.256	15.604	38.315
5	Ur-30/14*/black shale	3.50	13.00	2.20	19.4356	15.6837	40.0594	18.225	15.605	38.312
6	B-3/ same	17.31	12.17	2.62	18.6190	15.6357	38.8206	18.342	15.630	37.963
7	KS-a/ same	20.3	12.0	2.6	18.6181	15.6285	38.7395	18.363	15.623	38.435
8	D-1/ same	25.5	11.9	2.6	18.5535	15.6355	38.6791	18.402	15.618	38.415

* – data from (Lebedev et al., 2018).

(Gavrilov, 2005). In total, the stratigraphic and geochronological data allow us to limit the age range of magmatism of the Khulam Complex to the late Bajocian–Bathonian, i.e., 169–166 Ma.

As noted above, the ore mineralization at the Raduzhnoe Au–sulfide deposit developed directly in Paleozoic granitoids, Bajocian terrigenous strata, and trachytes–rhyolites of hypabyssal intrusions of the Khulam Complex. Consequently, the lower age limit of the deposit should also be accepted as Late Bajocian–Bathonian. On the other hand, the Callovian sediments present in the region have not been subjected to metasomatic alterations. Accordingly, the formation of ores of the Raduzhnoe deposit occurred before the Callovian.

Thus, we can conclude that the Raduzhnoe deposit formed in the Late Bajocian–Bathonian, synchronously with the moderately alkaline magmatism of the Khulam Complex or immediately after its termination.

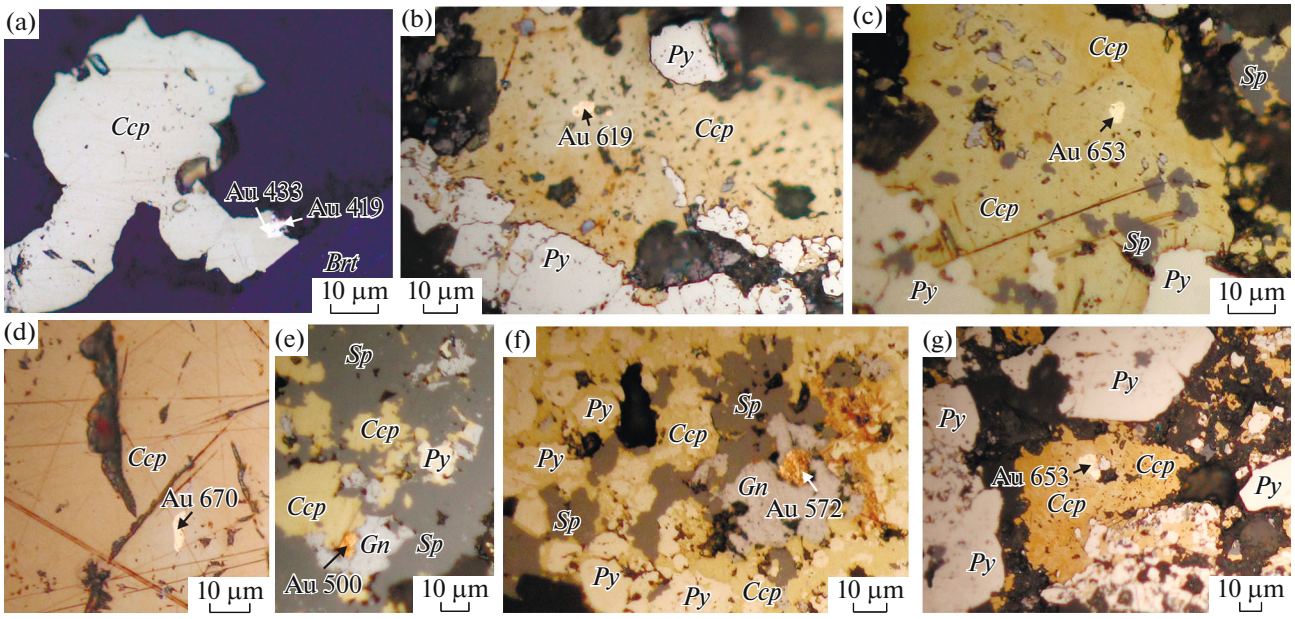

Fig. 11. Native gold in chalcopyrite (*Ccp*) and galena (*Gn*), gold-sulfide assemblage (chalcopyrite, pyrite *Py*, galena, sphalerite *Sp*). Pervaya ore zone, borehole 3001. Polished thin sections. Numerals, gold fineness. (a) Sample 3001/2; (b, c, d, g) sample 3001/4; (e, f) sample 3001/5.

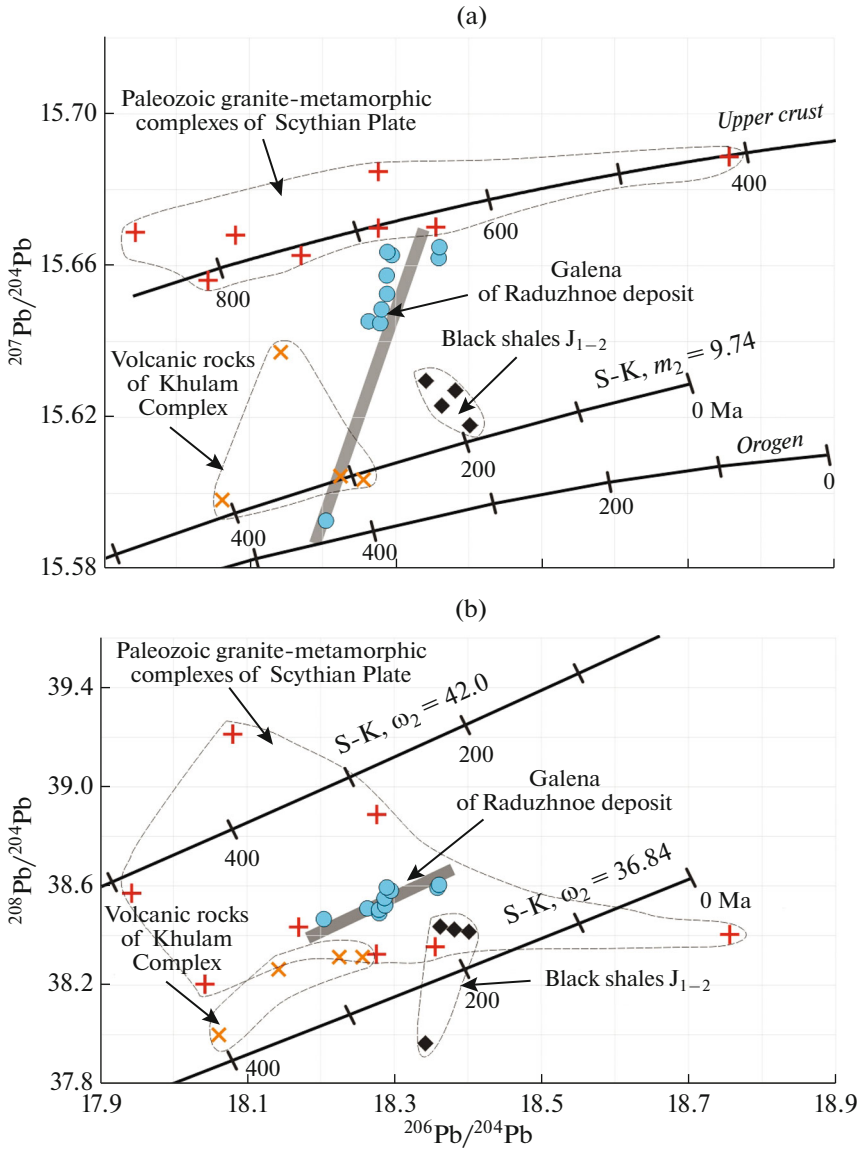

Fig. 12. Pb isotope diagrams for galena from gold ore mineralization of Au–sulfide Raduzhnoe deposit, as well as host ores of Paleozoic magmatic and metamorphic formations, Jurassic volcanic rocks of Khulam Complex, and black shales. Data on Paleozoic rocks of crystalline basement of tectonic zone of Main Caucasian Range were used (Lebedev et al., 2010, 2018).

Type of Ore Mineralization

There are different views on the genesis of the Raduzhnoe deposit. According to (Lezin et al., 1976(ar); Kurbanov et al., 2004(ar)), this deposit is attributed to the gold–silver epithermal type. One of the main criteria for distingushing this type is the presence of adularia in argillized rhyolites. Our petrographic studies revealed no hydrothermal adular in ores. In addition, the Raduzhnoe deposit differs from typical gold–silver deposits, which are attributed to LS-type ores based on the widespread occurrence of sulfides (<2 vol % in LS-type ores) and absence of typical colloform textures.

The intensive development of gypsum–anhydrite mineralization, essentially sulfide composition of ores, and subsheet shape of orebodies have allowed some authors (Kryazhev and Dvurechenskaya, 2014(ar)) to attribute the Raduzhnoe deposit to the Kuroko polymetallic–sulfide type. However, sulfide deposits on the northern slope of the Greater Caucasus (Urup, Khudes, etc.), attributed by G.V. Ryabov and I.A. Bogush (2012) to the Urals type, are spatially and genetically related to Devonian volcanism and are located north of Tyrnyauz–Pshekish suture zone in the Front Range tectonic zone. It is also known that anhydrite (Hedenquist et al., 2000) is attributed to typical vein minerals of IS-type deposits.

The absence of minerals characteristic of high-sulfidation (HS) type (pyrophyllite, alunite, etc.) among metasomatic rocks, signs of replacement of epithermal epidote-free chlorite propylites by epithermal argillizated rocks, and widespread mixed-layer minerals of the illite–smectite group make it possible to to attribute wallrock metasomatic rocks of the Raduzhnoe deposit to epithermal argillisites characteristic of most low-sulfidation (LS) and intermediate-sulfidation (IS) deposits (Einaudi et al, 2003).

Given the mineral composition of ores (pyrite, chalcopyrite, sphalerite, galena, Ag-bearing tetrahedrite-(Zn), and tennantite-(Fe,Zn)), spatiotemporal and, as shown below, genetic assemblages with bimodal continental postcollisional magmatism, as well as the low fineness of native gold, the Raduzhnoe deposit can be attributed to the IS epithermal type (Sillitoe et al, 2003). Such objects are usually characterized by lower Au contents than LS deposits (Wang et al., 2019).

Following the classification of (Wang et al., 2019), IS-type deposits are further divided into two subtypes: neutral-compressional (NC) and extensional (E). NC subtype deposits are formed in a compressional setting or in subneutral stress setiings, which are represented by magmatic arcs that developed at the subduction stage (in particular, continental arcs and mature island arcs). E-subtype deposits are characterized by a close relationship with highly differentiated felsic volcanic rocks, which is also typical of the Bezengi ore district, where the ore mineralization is associated with felsic igneous rocks of the Khulam Complex. In turn, NC-subtype deposits are associated with more mafic volcanic rocks. Thus, it can be suggested that the Bezengi ore district and Raduzhnoe deposit in particular belong to the E subtype of IS deposits.

According to existing ideas (Korolkov, 2007), the postcollisional geotectonic setting in which the Raduzhnoe deposit supposedly formed, is characterized by block movements along fault zones and active volcanic activity with the formation of ore-bearing moderately alkaline magmatic complexes of various composition. The tectonic evolution at this stage is usually described as strike-sleep tectonics, when folded deformations were of subordinate importance. In some cases, local extension zones began to develop in a rifting setting. For example, postcollisional high-potassic magmatism is described in the Ulaan-Jiawula metallogenic province of East Asia (Nie et al., 2015); large Ag–Pb–Zn deposits are paragenetically related to this province (e.g., the Tsav, Noyon-Tologoi, etc.). (Gantumur et al., 2010; Chugaev et al., 2013)). The Tsav deposit can be called the most similar to the Raduzhnoe deposit in genetic type, pattern of magmatism, and mineralogical composition of ores.

Lead Sources for Gold Ore Mineralization of the Raduzhnoe Deposit

The correlation dependences revealed for lead from galena, $^{206}Pb/^{204}Pb$–$^{207}Pb/^{204}Pb$, on the one hand, and $^{206}Pb/^{204}Pb$–$^{208}Pb/^{204}Pb$, on the other, are expressed as short trends (Fig. 12). They indicate the participation of at least two sources that differ in their Pb isotopic characteristics, which are most clearly expressed in the $^{207}Pb/^{204}Pb$ ratio and μ_2 parameter.

Using the Stacey-Kramers two-stage model, the Pb isotopic data obtained for galena make it possible to estimate some parameters of the lead sources of the Raduzhnoe gold ore deposit.

According to these evaluations, the main source had elevated (with recpect to average crustal) values: $\mu_2 = {}^{238}U/^{204}Pb = 9.91–9.99$, $\omega_2 = {}^{232}Th/^{204}Pb = 38.9–40.5$ and $Th/U = 4.00–4.05$ (Table 5). These parameters are typical of rocks of sialic continental crust. In turn, the Pb–Pb model age (Tm), which reflects the time of Pb separation from the U–Th–Pb isotope system of the source, is almost two times older (Tm = 302–381 Ma) than the age of the deposit assumed from geochronological data. This discrepancy indicates a complex (multistage) evolution of ore lead in this reservoir, including a change (decrease) in the U/Pb ratio. In general, the model parameters μ_2, ω_2, Th/U, and Tm give grounds to suggest entry of Pb into the ore-forming system from a crustal source.

According to the Zartman–Doe model, the considered source of ore lead, characterized by high $^{207}Pb/^{204}Pb$ (≥15.67) and μ_2 (≥9.9) values, is close to the Paleozoic upper crustal reservoir (Fig. 12). Black shales differ significantly in their Pb-isotope characteristics from the proposed source. The field of the point data of these rocks in both diagrams lies to the right of the trend of galena points from ore formations (Fig. 12). Due to this, we can exclude them from further discussion.

Outcrops of Paleozoic granitic and metamorphic rocks are widespread within the tectonic zone of the Greater Caucasian Range. According to some researchers (Leonov et al., 2007), these rocks belong to the crystalline basement of the epi-Hercynian Scythian Plate. Based on a geophysical survey performed in the area of the Raduzhnoe deposit, the Jurassic volcanogenic-sedimentary complexes cover the Paleozoic upper crustal formations, about 30 km thick an average (Shempelev et al., 2005). This makes it possible to consider them a potential source of ore lead. To assess the role of this reservoir in the genesis of the Au–sulfide mineralization, previously obtained data on the Pb isotopic composition of Paleozoic granitoids and metamorphic schists of the Greater Caucasus Range (Lebedev et al., 2010, 2018), corrected to an age of 167 Ma ago, were plotted on the Pb diagrams (Fig. 12). The data points show significant scatter in the diagrams, indicating heterogeneity of the

crystalline basement rocks in terms of Pb isotopic composition, Th/U ratio, and, to a lesser extent, U/Pb ratio (Fig. 12). On the uranogenic isotope Pb diagram (Fig. 12), the field of Paleozoic rocks extends along the upper crustal evolution curve of the Zartman–Doe model and is located on the upper continuation of the trend, formed by points of for galena from gold mineralization. Data points of Paleozoic rocks in the $^{206}Pb/^{204}Pb$–$^{208}Pb/^{204}Pb$ diagram form a wide field between the Stacey–Kramers evolution curves with the parameters $\omega_2 = 36.84$ at Th/U = 3.78 and $\omega_2 = 42$ at Th/U = 4.31. All galena data points, as well as most points of volcanic rocks of the Khulam Complex and black shales, also fall into this field. Thus, the observed correlation between the Pb isotopic composition in ores and Paleozoic basement rocks gives reason to consider the latter as the main Pb source at the Raduzhnoe deposit.

This conclusion is also supported by the above parameters of the ore lead source ($\mu_2 \geq 10$, $\omega_2 \geq 41$, and Th/U ≥ 4.1), as well as more ancient Pb–Pb model dates compared to the age of the deposit itself. These features are characteristic of the continental crust that experienced metamorphic transformation and partial melting accompanied by the generation of granitoid melts. As a result of these processes, the Th/U and Th/Pb ratios increase and the U/Pb ratio decreases in the crust (Taylor and McLennan, 1985). The Late Paleozoic model Pb–Pb ages obtained for this source of lead can be explained by a decrease in the U/Pb ratio in the crust shortly before ore-forming processes.

Another source of ore lead had relatively low $^{207}Pb/^{204}Pb$ (≤15.60) ratio (≤15.60) and μ_2 parameter (≤9.7) values. According to these characteristics, the volcanic rocks of the Khulam Complex are the closest to this source. In addition, as noted above, the fields of data points of these volcanic rocks in both diagrams lie on the lower continuation of the ore lead trend. In total, the features of the Pb isotopic composition of ore and volcanic rocks allow the conclusion that the same source of lead could have taken part in the gold-bearing mineralization and magmatic melts of the Khulam Complex.

The observed enhanced scatter of data points along the mixing trend in the Pb isotope diagrams (Fig. 12) is primarily a consequence of the primary Pb-isotope heterogeneity of the crystalline basement rocks and, to a lesser extent, of the volcanic rocks of the Khulam Complex. The latter are considered to be the two main sources of ore lead. This explanation does not suggest that lead comes from other additional reservoirs.

The geochemical data are consistent with the results of Pb isotopic studies. Table 7 demonstrates that only the Paleozoic granite-metamorphic formations and some felsic rock varieties of the Khulam Complex of all possible geochemical reservoirs—potential sources of ore lead present in the Raduzhnoe deposit, have elevated Pb content as compared to the clarke values.

Role of Middle Jurassic Volcanism of the Khulam Complex in the Genesis of Gold-Ore Mineralization

As shown above, in many cases, the Au–sulfide mineralization within the Bezengi ore district was overprinted directly on the felsic volcanic rocks of subvolcanic bodies of the Khulam Complex (both rhyolites and trachytes) and formed either synchronously or immediately after termination of endogenic activity in the region. Ore mineralization is often localized in the contact zones of intrusions, which may indicate at least a paragenetic relationship between Au–sulfide mineralization formation processes and volcanic activity. Lastly, the isotope-geochemical data that we obtained and examined in detail demonstrate that the ore lead at the Raduzhnoe deposit is of mixed origin (Fig. 12). At the same time, we can suggest that the igneous rocks of the Khulam Complex and ores had the same Pb source. This allows us to speak with a great degree of certainty about emplacement of the Au–sulfide mineralization synchronously with Middle Jurassic magmatism of the Khulam Complex (ca. 167 Ma ago).

As shown previously (Kaigorodova and Lebedev, 2022), the petrological and geochemical characteristics of the igneous rocks (both felsic and mafic varieties) of the Khulam Complex are close to the typical intraplate continental formations. The concentrations of most ore elements (Ni, Co, Cr, V, Mo, W, Sn, Sb, Zn, Cd) are at the level of clarke values except for Ag and Au (Solovov et al., 1990). The Ag and Au contents (Table 7) significantly exceed clarke values estimated for rocks with the corresponding composition (Ag in mafic rocks, 0.3–1.3 ppm; Ag in felsic rocks, 0.6–3.6 ppm; Au in all types of rocks, 0.1–1.0 ppm). This allows us to consider the magmatism of the Khulam Complex as ore-bearing. The role of the host black shales in the formation of the deposit is controversial. According to the results of studying black shales, which could be a potential Au source, the Au content in them is below the ICP-MS method detection limit (0.001 ppm). Nevertheless, the role of black shales in the formation of the deposit requires further investigation.

Table 7 shows that the Paleozoic formations, primarily, crystalline schists, could be the most probable potential source of Cu, as well as was shown for Pb, in the sulfide mineralization of the Raduzhnoe deposit. In turn, the Jurassic black shales were, most likely, a source of Zn, the concentration of which noticeably exceeds bulk Earth values. However, the participation of other geochemical reservoirs—Paleozoic upper crustal and Jurassic magmatic—cannot be excluded.

Fractional crystallization (FC), which played a leading role in rock formation in the volcano-plutonic

Table 7. Contents of main ore elements in geochemical reservoirs at Raduzhnoe deposit and clarke values for rocks of corresponding composition (according to Solovov et al., 1990)

Geochemical reservoir	Au, ppm	Ag, ppm	Pb, ppm	Zn, ppm	Cu, ppm
Khulam Complex (J_2), felsic rocks	**0.4–1.7** (n = 12)	**0.3–8.9** (n = 16)	1–**60** (n = 17)	17–**93** (n = 18)	2–22 (n = 17)
Clarke value	*0.004*	*0.05*	*20*	*60*	*20*
Khulam Complex (J_2), intermediate–felsic rocks	**0.3–0.5** (n = 3)	**1.4–3.5** (n = 4)	2–8 (n = 4)	18–**117** (n = 5)	5–30 (n = 4)
Clarke value	*0.003*	*0.1*	*10*	*72*	*55*
Khulam Complex (J_2), mafic rocks	**0.1** (n = 1)	**0.4–1.3** (n = 4)	3–10 (n = 8)	68–82 (n = 8)	33–75 (n = 8)
Clarke value	*0.004*	*0.1*	*8*	*110*	*100*
Black shales (J_2)	<0.001 (n = 5)	0.01–0.03 (n = 5)	17–25 (n = 5)	**125–157** (n = 5)	29–35 (n = 5)
Clarke value	*0.001*	*0.1*	*20*	*90*	*60*
Granites PZ	<0.001*	0.01–0.03 (n = 6)	8–**46** (n = 11)	20–**90** (n = 11)	2–11 (n = 11)
Clarke value	*0.004*	*0.05*	*20*	*60*	*20*
Metamorphic schists and gneisses PZ	<0.001*	0.06 (n = 1)	11–55 (n = 4)	40–**170** (n = 4)	11–**81** (n = 4)
Clarke value	*0.004*	*0.05*	*20*	*100*	*43*

contents, exceeding clarke values, in rocks of corresponding composition are shown in bold. *Au content in Paleozoic basement rocks is from (Stativkin and Stativkina, 1976(ar), etc.).

Khulam Complex (Kaigorodova and Lebedev, 2022) resulted in significant enrichment of felsic volcanic rocks in some incompatible REE elements (Zr, up to 2600 ppm; Nb, up to 300 ppm; Ta, up to 30 ppm; Ce, up to 400 ppm). Thus, the FC processes that contributed to the formation of a bimodal assemblage of the volcano-plutonic Khulam Complex determined the REE—rare metal specialization (Zr, Nb, Ta) of trachytes and rhyolites.

In considering the genetic assemblage of Au ore mineralization at the Raduzhnoe deposit with the magmatic activity of the volcano-plutonic Khulam Complex suggested by some researchers (Kalinin et al., 1979(ar), Koptyukh et al., 1985(ar)), analysis of the petrological and geochemical characteristics of the studied volcanic rocks confirms that this complex should be considered ore-bearing. It can be assumed that felsic melts, which were probably significantly enriched in volatile components (as evidenced, in particular, by large-scale autometamorphic alteration of rhyolites), initiated significant hydrothermal activity within the area of volcanic activity. This is indicated by the spatial and structural assemblage of ore mineralization with magmatic formations of the Khulam Complex.

CONCLUSIONS

The mineral composition of ores (pyrite, chalcopyrite, sphalerite, galena, and fahlore) and the relationship of the deposit with bimodal continental postcollisional magmatism and low fineness of native gold (419–670‰) indicate that the Raduzhnoe ore deposit can be attributed to the E-subtype (after Wang et al., 2019) of epithermal intermediate-sulfidation deposits, according to the classification (Sillitoe and Hedenquist, 2003). Taking into account the total geological, isotopic-geochemical, and petrological-geochemical data available, we can suggest that the deposit was formed in the Middle Jurassic simultaneously with manifestation of moderately alkaline magmatism of the Khulam Complex (~167 Ma).

The results of studying the Pb isotopic composition of galena from the Au–sulfide mineralization of the Raduzhnoe deposit indicate the mixed origin of this component in ores. Paleozoic granitoids and metamorphic complexes that make up the upper crust in the region and are generally characterized by a higher Pb content were the main source of Pb. Extraction of Pb from upper crustal strata occurred most likely due to the action of hydrothermal solutions during the Middle Jurassic magmatism with elevated alkalinity (Khulam Complex). As evidenced by a linear trend of mixture formed by all data points of the studied galena, another source of ore lead of secondary importance were hydrothermal solutions produced by Khulam Complex magmatism. The end compositions of this trend are located in the fields of Paleozoic basement rocks and volcanic rocks of the Khulam Complex. The petrological and geochemical characteristics

of the rocks of the Khulam Complex discussed in (Kaigorodova and Lebedev, 2022) suggest that this (magmatic) source of lead, which participated in the genesis of both volcanic rocks and ores of the Raduzhnoe deposit, has a deep origin and was represented by enriched mantle melt with close-to-E-MORB geochemical parameters.

Because the magmatic formations of the Khulam Complex (both mafic and felsic) are characterized by elevated Ag and Au concentrations exceeding the clarke values by an order of magnitude, we can suggest that the source of these elements in the ores of the Bezengi ore district is hydrothermal solutions produced due to Middle Jurassic magmatism with elevated alkalinity. To confirm this hypothesis, further research is necessary, including a study of the Ag isotopic composition in sulfides and rocks of the Khulam Complex.

The low Cu and Zn concentrations in felsic rocks of the Khulam Complex indicate that the hydrothermal solutions associated with Middle Jurassic magmatism were hardly the main source of chalcophile elements in the ores of the Raduzhnoe Au–sulfide deposit. Most likely, they were taken from the host terrigenous Jurassic strata or metamorphic rocks and granitoids of the Paleozoic basement.

ACKNOWLEDGMENTS

The authors are grateful to A.F. Baranovsky, chief geologist of Kabardino-Balkarian Geological Survey Expedition, and V.P. Davidenko, geologist, for their help in field works, as well as to N.G. Lyubimtseva for assitance in studying the mineralogy of the deposit.

FUNDING

The study was supported by the Ministry of Science and Higher Education of the Russian Federation (grant no. 13.1902.21.0018 "Fundamental Problems of Development of the Mineral and Raw Materials Base for Russia's High-Tech and Power Industries").

CONFLICT OF INTEREST

The author declares that he has no conflict of interest.

REFERENCES

Beznosov, N.V., Burshtar, M.S., Vakhrameev, V.A., Krymgol'ts, G.Ya., Kutuzova, V.V., Rostovtsev, K.O., and Snegireva, O.V., *Ob"yasnitel'naya zapiska k stratigraficheskoi skheme yurskikh otlozhenii Severnogo Kavkaza* (Explanatory Note to the Stratigraphic Scheme of the Jurassic Deposits of North Caucasus), Moscow: Nedra, 1973.

Biagioni, C., George, L.L., Cook, N.J., Makovicky, E., Moelo, Y., Pasero, M., Sejkora, J., Stanley, C.J., Welch, M.D., and Bosi, F., The tetrahedrite group: nomenclature and classification, *Am. Mineral.: J. Earth Planet. Mater.,* 2020, vol. 105, no. 1, pp. 109–122.

Borsuk, A.M., Tsvetkov, A.A., and Lezin, S.I., Propylitized rocks of Gornaya Balkaria, North Caucasus) and related ore mineralization, *Izv. Akad. Nauk SSSR, Ser. Geol.,* 1977, no. 11, pp. 37–52.

Chernyshev, I.V., Chugaev, A.V., and Shatagin, K.N., High-precision Pb isotope analysis by multicollector-ICP-mass-spectrometry using $^{205}Tl/^{203}Tl$ normalization: optimization and calibration of the method for the studies of Pb isotope variations, *Geochem. Int.,* 2007, vol. 45, no. 11, pp. 1065–1076.

Chernyshev, I.V., Chugaev, A.V., Bortnikov, N.S., Gamyanin, G.N., and Prokopiev, A.V., Pb isotopic composition and metal sources of Au and Ag deposits of the South Verkhoyansk region (Yakutia, Russia) according to high-precision MC-ICP-MS data, *Geol. Ore Deposits,* 2018, vol. 60, no. 5, pp. 398–417.
https://doi.org/10.1134/S1075701518050033

Chudnenko, K.V. and Palyanova, G.A., Thermodynamic modeling of native formation of Au–Ag–Cu–Hg solid solutions, *Appl. Geochem.,* 2016, vol. 66, pp. 88–100.

Chugaev, A.V., Chernyshev, I.V., Bortnikov, N.S., Kovalenker, V.A., Kiseleva, G.D., and Prokof'ev, V.Yu., Lead isotope ore provinces of Eastern Transbaikalia and their relationships to regional structures: results of high-precision MC-ICP-MS study of Pb isotopes, *Geol. Ore Deposits,* 2013, vol. 55, no. 4, pp. 245–255.

Chugaev, A.V., Chernyshev, I.V., Lebedev, V.A., and Eremina, A.V., Lead isotope composition and origin of the Quaternary lavas of Elbrus Volcano, the Greater Caucasus: high-precision MC-ICP-MS data, *Petrology,* 2013, vol. 21, no. 1, pp. 16–27.

Chugaev, A.V., Plotinskaya, O.Yu., Dubinina, E.O., Sadasyuk, A.S., Gareev, B.I., Kossova, S.A., and Batalin, G.A., Crustal source of Pb and S at the Yubileynoe porphyry gold deposit (Southern Urals, Kazakhstan): high precision Pb–Pb and $\delta^{34}S$ data, *Geol. Ore Deposits,* 2021, vol. 63, no. 3, pp. 173–184.

Cohen, K.M., Finney, S.C., Gibbard, P.L., and Fan, J.-X., The ICS international chronostratigraphic chart, *Episodes,* 2013, vol. 36, pp. 199–204.

Dolgikh, A.G., Mesocenozoic magmatism of North Caucasus, *Mater. dokladov II regional'nogo petrograficheskogo soveshchaniya po Kavkazu, Krymu i Karpatam* (Proc. Reports of 2nd Regional Petrographic Conference on Caucasus, Crimea, and Carpathians), Tbilisi, 1978, pp. 173–179.

Gantumur, Kh., Batulzii, D., and Lkhamsuren, Zh., Geological characteristics and ore-forming solutions of the Tsav silver–lead–zinc deposits in northeastern Mongolia, *Izv. SO Sekts. Nauk o Zemle RAEN,* 2010, vol. 36, no. 1, pp. 12–22.

Gavrilov, Yu.O., *Dinamika formirovaniya yurskogo terrigennogo kompleksa Bol'shogo Kavkaza: sedimentologiya, geokhimiya, postsedimentatsionnye preobrazovaniya* (Dynamics of Formation of the Jurassic Terrigenous Complex of the Greater Caucasus: Sedimentology, Geochemistry, and Postsedimentary Transformations), Moscow: GEOS, 2005.

Gazeev, V.M., Gurbanov, A.G, and Kondrashov, I.A., Mafic rocks of the Middle Jurassic back-arc dike belt of the Greater Caucasus (geochemistry, petrogenetic problems, and geodynamic typification), *Geol. Geofiz. Yuga Rossii,* 2018, no. 2, pp. 16–29.

Gazeev, V.M., Gurbanov, A.G, and Kondrashov, I.A., Mesozoic subalkaline rocks of central Northern Caucasus: geodynamic typification, geochemistry, and metallogeny, *Geol. Geofiz. Yuga Rossii,* 2019, vol. 9, no. 3, pp. 48–62.

GIS-atlas (paket operativnoi geologicheskoi operatsii). Severo-Kavkazskii Federal'nyi Okrug (GIS-Atlas. (A Package of

Operative Geological Information), Northern Caucasian Federal Okrug), MPR RF. Fed. Agenstvo po Nedropol'zov., VSEGEI, 2020. http://atlaspacket.vsegei.ru.

Gurbanov, A.G., Gazeev, V.M., Leksin, A.B., Dokuchaev, A.Ya., Gol'tsman, Yu.V., Oleinikova, T.I., and Gurbanova, O.A., Paleogeodynamic reconstructions and metallogeny of the Early Jurassic Fiagdon mafic–ultramafic complex (Republic of North Ossetia–Alania), RF): petrochemical, geochemical, and isotope data, *Geol. Geofiz. Yuga Rossii,* 2017, no. 4, pp. 22–38.

Hedenquist, J.W., Arribas, A.R., and Gonzales-Urien, E., Exploration for epithermal gold deposits, *Rev. Econ. Geol.,* 2000, vol. 13, pp. 245–277.

Kaigorodova, E.N., Lebedev, V.A., Chernyshev, I.V., and Yakushev, A.I., Neogene–Quaternary magmatism in eastern Balkaria (North Caucasus, Russia): Evidence from the isotope–geochronological data, *Dokl. Earth Sci.,* 2021, vol. 496, no. 1, pp. 37–44.
https://doi.org/10.1134/S1028334X21010098

Kaigorodova, E.N. and Lebedev, V.A., The age, petrological-geochemical characteristics, and origin of igneous rocks of the Middle Jurassic Khulam volcano-plutonic complex, North Caucasus, *J. Volcanol. Seismol.,* 2022, vol. 16, no. 2, pp. 116–142.

Korol'kov, A.T., *Geodinamika zolotorudnykh raionov yuga Vostochnoi Sibiri* (Geodynamics of Gold Districts of the Southern East Siberia), Irkutsk: Irkut. Gos. Univ., 2007.

Le Bas, M.J., Le Maitre, R.W., Streckeisen, A., and Zanettin, B., A chemical classification of volcanic rocks based on the alkali–silica diagram, *J. Petrol.,* 1986, vol. 27, pp. 745–750.

Lebedev, A.P., Jurassic volcanogenic formation of Central Caucasus, *Tr. IGN AN SSSR,* 1950, vol. 113, 1950.

Lebedev, V.A., Chernyshev, I.V., Chugaev, A.V., Gol'tsman, Yu.V., and Bairova, E.D., Geochronology of eruptions and parental magma sources of Elbrus Volcano, the Greater Caucasus: K–Ar and Sr–Nd–Pb isotope data, *Geochem. Int.,* 2010, vol. 48, no. 1, pp. 41–67.

Lebedev, V.A., Chugaev, A.V., Vashakidze, G.T., and Parfenov, A.V., Formation stages and ore matter sources of the Devdoraki copper deposit, Kazbek volcanic center, the Greater Caucasus, *Geol. Ore Deposits,* 2016, vol. 58, no. 6, pp. 465–484.

Lebedev, V.A, Chugaev, A.V., and Parfenov, A.V., Age and ore matter sources of Au-sulfide mineralization of the Tanadon deposit, Republic of North Ossetia–Alania, Greater Caucasus, *Geol. Ore Deposits,* 2018, vol. 60, no. 4, pp. 328–346.

Leonov, Yu.G., Demina, L.I., Kopp, M.L., Koronovsky, N.V., Leonov, M.G., Lomize, M.G., Panov, D.I., Somin, M.L., and Tuchkova, M.I., *Bol'shoi Kavkaz v Al'piiskuyu epokhu* (Greater Caucasus in the Alpine Epoch) Moscow: GEOS, 2007.

Metasomatizm i metasomaticheskie porody (Metasomatism and Metasomatic Rocks), Moscow, Nauchnyi mir, 1998.

Naumov, E.A. Types of Gold Mineralization of the Altai-Sayan Fold Orogenic Area and Physicochemical Conditions of their formation, *Extended Abstract of Candidate's (Geol.-Min.) Dissertation,* Novosibirsk, 2007.

Nie, F.J., Li, Q.F., Liu, C.H., and Ding, C.W., Geology and origin of Ag–Pb–Zn deposits occurring in the Ulaan–Jiawula metallogenic province, northeast Asia, *J. Asian Earth Sci.,* 2015, vol. 97, pp. 424–441.

Pearce, J.A., *A user's guide to basalt discrimination diagrams. Trace element geochemistry of volcanic rocks: Applications for massive sulphide exploration, Geological Ass. Canada. Short Course Notes,* 1996, vol. 12, pp. 79–113.

Pis'mennyi, A.N., Tereshchenko, V.V., and Perfil'ev, V.A., *Gosudarstvennaya geologicheskaya karta Rossiiskoi Federatsii masshtaba 1 : 200000. Listy K-38-VIII, XIV (Sovetskoe),* (State Geological Map of the Russian Federation on a Scale 1 : 200000. Sheets K-38-VIII, XIV (Sovetskoe)), St. Petersburg: VSEGEI: 2002.

Ryabov, G.V. and Bogush I.A., Typification of sulfide deposits of Northern Caucasus, *Izv. Vyssh. Ucheb. Zaved., Severo-Kavkazsk. Region. Tekhnicheskie nauki,* no.5. 2012, pp. 88–91.

Sack, R.O. and Ebel, D.S., As–Sb exchange energies in tetrahedrite–tennantite fahlores and bournonite–seligmannite solid solutions, *Mineral. Mag.,* 1993, vol. 57, pp. 635–642.

Sack, R.O. and Loucks, R.R., Thermodynamic properties of tetrahedrite–tennantite: constraints on the interdependence of the Ag–Cu, Fe–Zn, Cu–Fe, and As–Sb exchange reactions, *Am. Mineral.,* 1985, vol. 70, nos. 11–12, pp. 1270–1289.

Sharpenok, L.N., Kukharenko, E.A., and Kostin, A.E., *Endogennye rudonosnye brekchievye obrazovaniya. Metodicheskie rekomendatsii po vyyavleniyu endogennykh brekchievykh obrazovanii razlichnykh geneticheskikh tipov i otsenke ikh potentsial'noi rudonosnosti primenitel'no k zadacham Gosgeolkart* (Endogenous Ore-Bearing Brecciated Rocks. Methodical Recommendations on Revealin Endogenous Brecciated Rocks of Different Genetic Types in Assessment of their Ore Potential as Applied to the Gosgeolkarta Tasks), St. Petersburg: VSEGEI, 2018.

Shempelev, A.G., P'yankov, V.Ya., Lygin, V.A., Kukhmazov, S.U., and Morozova, A.G., Results of geophysical studies along the Elbrus profile (Elbrus Volcano–Caucasian Mineral Waters), *Regional. Geol. Metallogen.,* 2005, no. 25, pp. 178–185.

Sillitoe, R.H. and Hedenquist, J.W., Linkages between volcanotectonic settings, ore-fluid compositions, and epithermal precious metal deposits, *Soc. Econ. Geol. Spec. Publ.,* 2003, vol. 10, pp. 1–29.

Solovov, A.P., Arkhipov, A.Ya., Bugrov, V.A., Vorob'ev, S.A, Geriman, D.M., Grigoryan, S.V., Kvyatkovskii, E.M., Matveev, A.A., Milyaev, S.A., Nikolaev, V.A. Perel'man, A.I., Shvarov, Yu.V., Yufa, B.Ya., and Yaroshevskii, A.A., *Spravochnik po geokhimicheskim poiskam poleznykh iskopaemykh* (A Textbook on the Geochemical Prospecting of Mineral Resources), Moscow: Nedra, 1990.

Somin, M.L., Pre-Jurassic basement of the Greater Caucasus: brief overview, *Turk. J. Earth Sci.,* 2011, vol. 20, pp. 545–610.

Stacey, J.S. and Kramers, J.D., Approximation of terrestrial lead isotope evolution by a two-stage model, *Earth Planet. Sci. Lett.,* 1975, vol. 26, pp. 207–221.

Taylor, S.R. and McLennan, S.M., *The Continental Crust: its Composition and Evolution* Oxford: Blackwell, 1985.

Wang, L., Qin, K-Z., Song, G-X., and Li, G-M., A review of intermediate sulfidation epithermal deposits and subclassification, *Ore Geol. Rev.,* 2019, vol. 107, pp. 434–456.

Zartman, R.E. and Doe, B.R., Plumbotectonics—the model, *Tectonophysics,* 1981, vol. 75, pp. 135–162.
https://doi.org/10.1016/0040-1951(81)90213-4

Translated by D. Voroshchuk